Нуклеарна техника

Nuclear engineering and technology

Uticaj gama zračenja na mernu nesigurnost brzog, kompenzovanog kapacitivnog delila

Nenad Kartalović, Koviljka Stanković, *Member, IEEE*, Dušan Nikezić, Tomislav Stojić, Uzahir Ramadani i Uroš Kovačević

***Apstrakt*—U radu se razmatra uticaj gama zračenja na pouzdano merenje jednokratnih naponskih impulsa snopova elektrona za injektovanje u plazmu tokom fuzionih eksperimenata. U tu svrhu je konstruisano brzo, 10 GHz, delilo napona. Visokonaponski kondenzator je bio gasni kondenzator, a niskonaponski kondenzator je bila paralelna veza 10 liskunskih kondenzatora. Pokazalo se da primljena doza zračenja ispravlja prenosni odnos pošto poravnjava frekventnu karakteristiku liskuna u oblasti prostornog naelektrisanja. Ova pojava je objašnjena i sa pozitivnog i sa negativnog aspekta sa efektom na konkretnu primenu. Takođe je ukazano na potrebu daljeg rada na ovom problemu u cilju ustanovljavanja saturacione doze za dobijanje konstantne frekventne karakteristike liskuna. Istaknut je i interes za ponašanje brzog delila u neutronskom polju.**

***Ključne reči*— fuzioni eksperiment; merenje naponskog talasa brzine 10 GHz; brzi delitelj napona; uticaj doze gama zračenja na tačnost i ponovljivost merenja.**

I. Uvod

SADAŠNJA koncepcija fuzionog reaktora se zasniva u zagrevanju plazme čestičnim snopovima (pošto se pokazalo da plazma nakon usijanja počne da reflektuje laserski snop koji je dugo bio predviđen za zagrevanje plazme). Čestice kojima se injektuje energija u plazmu smeštenu u „magnetnoj boci“ su elektroni. Ti elektroni se dobijaju standardnim Marksovim generatorom impulsnog oblika 1.2/50. Impulsi oblika 1.2/50 se sistemom provodnika i kondenzatora (kod kojih je i provodnik i dielektrik dejonizovana voda) pretvaraju u Hevisajdove (step) impulse širine oko 5 ns i snage više stotina GW. Pošto je ideja energetskih fuzionih postrojenja da desetak takvih elektronskih „topova“ istovremeno injektuju energiju od više TW u plazmu njihove najvažnije osobine su istovremenost okidanja (da nema jitera) i isti oblik izlaznog napona. Prvi problem se rešava troelektrodnim okidnim iskrištem, a drugi primenom brzih, kompenzovanih kapacitivnih sondi odnosno delitelja [1-5].

Pošto brzi, kompenzovani delitelji mere naponski oblik impulsa brzine nano sekunde i snage GW na njih deluje visokoenergetsko polje gama zračenja. Cilj ovog rada je da se odredi kako takvo polje gama zračenja deluje na pouzdanost merenja brzog, kompenzovanog kapacitivnog delila.

Nenad Kartalović – Elektrotehnički institut Nikola Tesla, Koste Glavinića 8a, 11000 Beograd, Srbija (e-mail: kartal@ieent.org).

Koviljka Stanković – Elektrotehnički fakultet, Univerzitet u Beogradu, Bulevar kralja Aleksandra 73, 11120 Beograd, Srbija. (e-mail: kstankovic@etf.rs).

Dušan Nikezić – Institut za nuklearne nauke „Vinča“ - Institut od nacionalnog značaja za Republiku Srbiju, Univerzitet u Beogradu, Mike Petrovića Alasa bb., 1100 Beograd, Srbija (e-mail: dusan@vin.bg.ac.rs).

Tomislav Stojić – Mašinski fakultet, Univerzitet u Beogradu, Kraljice Marije 16, 11120 Beograd, Srbija (e-mail: tstojic@mas.bg.ac.rs).

Uzahir Ramadani – Institut za nuklearne nauke „Vinča“ - Institut od nacionalnog značaja za Republiku Srbiju, Univerzitet u Beogradu, Mike Petrovića Alasa bb., 1100 Beograd, Srbija (e-mail: uzahir@vin.bg.ac.rs).

Uroš Kovačević – Inovacioni centar Mašinskog fakulteta, Kraljice Marije 16, 11120 Beograd, Srbija (e-mail: ukovacevic@mas.bg.ac.rs.

II. Kapacitivno delilo

Koeficijent delenja kapacitivnog delitelja, slika 1, u praksi je povezan sa spoljnim provodnicima i frekventnim karakteristikama dielektrika kondenzatora. Induktivnost spoljnih provodnika koji povezuju izvor napona i delitelja, u prvoj aproksimaciji može biti određena kao induktivnost konture koja iznosi oko 1 μH/m. U praksi se treba konstruisati merni sistem sa minimalnom induktivnošću. Generalno induktivnost u tehnici visokih napona predstavlja najveći problem pošto lako dovodi do oscilatornih, pa i rezonantnih pojava [6,7].

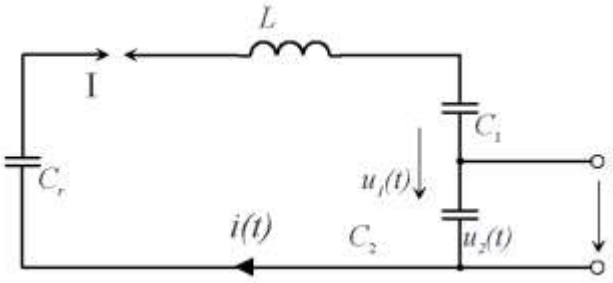

Sl. 1. Uprošćena zamenska šema kola pražnjenja generatora udarnog napona sa deliteljem; L - ukupna induktivnost kola pražnjenja.

Frekventna karakteristika je zavisnost dielektrične konstante od frekvencije. Frekventna karakteristika zavisi od tipa polarizacije materijala koji se koriste kao dielektrici kondenzatora (visokonaponskog i niskonaponskog) kod delila napona. Frekventna karakteristika je osnovni uzrok što mereni visoki napon (naročito ako je brz), nije u linearnom odnosu sa izmerenim naponom. To znači da je koeficijent prenosa (u najjednostavnijem obliku) funkcija frekvencije:

$$n = \frac{U_1}{U_2} = \frac{C_2(\omega)}{C_1(\omega)} = f(\omega) \qquad (1)$$

Na taj način razdelnik napona ima različite vrednosti koeficijenta prenosa za različite frekvencije što deformiše

izmerenu vrednost [8,9].

Pošto postoje elektronska, jonska i prostorna vrsta polarizacije realna i imaginarna komponenta dielektrične konstante izgleda kao na slici 2. U praksi, pri izradi kapacitivnog delila za frekvencije GHz treba dobro voditi računa o izboru pravog materijala za dielektrike kondenzatora. Pored toga pri tako visokom redu veličine brzine impulsnog napona u razmatranje se mora uzeti induktivnost i otpornost svih komponenti.

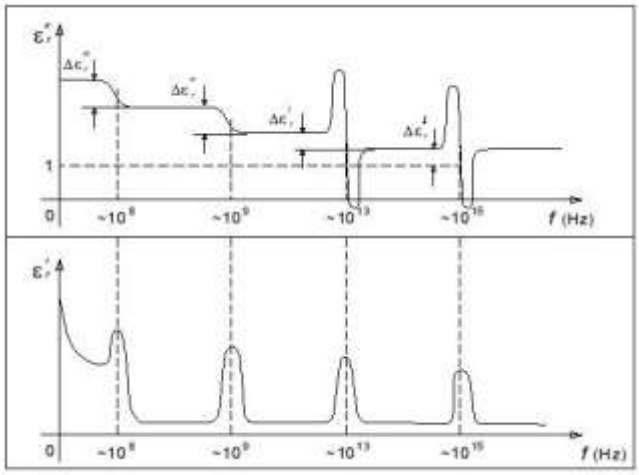

Sl. 2. Frekventna karakteristika materijala koji ima elektronski, jonski i prostorni tip polarizacije; εr“ je realna komponenta relativne dielektrične konstante, εr’ je imaginarna komponenta relativne dielektrične konstante.

Usled toga kapacitivni razdelnik ne izgleda više kao dva redno vezana kondenzatora, slika 3a, već kao složena struktura, slika 3b. Prema tome da bi se izradilo delilo napona sa kojim je moguće meriti izlaz iz fuzionog topa ono mora imati minimalnu otpornost i induktivnost komponenata, konstantne frekventne karakteristike u oblasti od 0 – 10 GHz. Pored svega toga delila za ovu namenu moraju biti u potpunosti otporna na polje gama zračenja širokog opsega (u kome rade) [10-14].

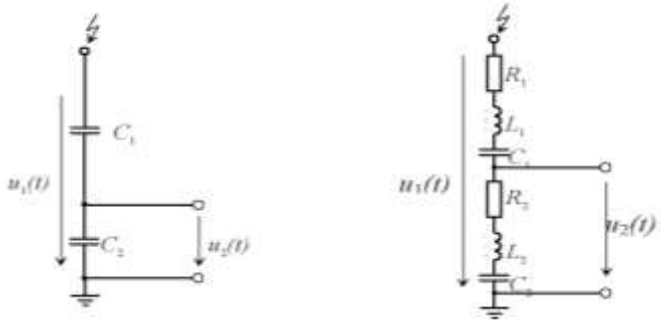

Sl. 3a. Kapacitivni delitelj napona sa skoncentrisanim kapacitetom u grani visokog napona; Slika 3b. Zamenska šema kapacitivnog delitelja napona uz uzimanje u obzir njegove induktivnosti i otpora.

III. EKSPERIMENT

Da bi se izbegli prethodno pobrojani neželjeni efekti napravljeno je brzo kapacitivno delilo sa gasnim visokonaponskim kondenzatorom tipa kalota-kalota. Spoljašnje i unutrašnje površine tog gasnog kondenzatora bile su polirane do visokog sjaja. Komora gasnog kondenzatora bila je napunjena SF6 gasom pod pritiskom 5 bar. Ovakvim izborom visokonaponskog kondenzatora izbegnuto je nepovoljno dejstvo elektrostatičkih i elektrodinamičkih sila (što se dešava u slučaju da je visokonaponski kondenzator tipa ulje-papir). Na slici 4 prikazano je telo visokonaponskog kondenzatora zajedno sa visokonaponskom kalotom [15,16].

Sl. 4. Fotografija kućišta delitelja napona.

Kao niskonaposnki kondenzator korišćena je paralelna veza od po deset identičnih liskunskih kondenzatora zalivenih u epoksilnu smolu. Korišćenje paralelne veze je omogućilo deset puta veći kapacitet (Ce = 10C) i deset puta manju induktivnost (Le = L/10). Na slici 5 prikazan je niskonaponski kondenzator korišćen u radu. Merni izvod između visokonaponskog i niskonaponskog kondenzatora bio je izrađen u obliku talasovodnog 50 Ω otpornika. Na gornjem kraju talasovodni otpornik je završavao na niskonaponskoj kaloti visokonaponskog kondenzatora. Na donjoj strani talasovodni otpornik je prolazio kroz niskonaponski kondenzator i završavao BNC buksnom. Talasovodni otpornik je primenjivan pošto je njegova otpornost jednaka prilagodnoj otpornosti od 50 (korišćeni su 50 Ω kablovi) a induktivnost je nula. Sve veze u niskonaponskom kondenzatoru su izrađene da dužinski budu minimalne.

Sl. 5. Fotografija niskonaponskog kondenzatora.

Na slici 6 je prikazan poprečni presek konstruisanog brzog, kompenzovanog kapacitivnog delitelja [17-19].

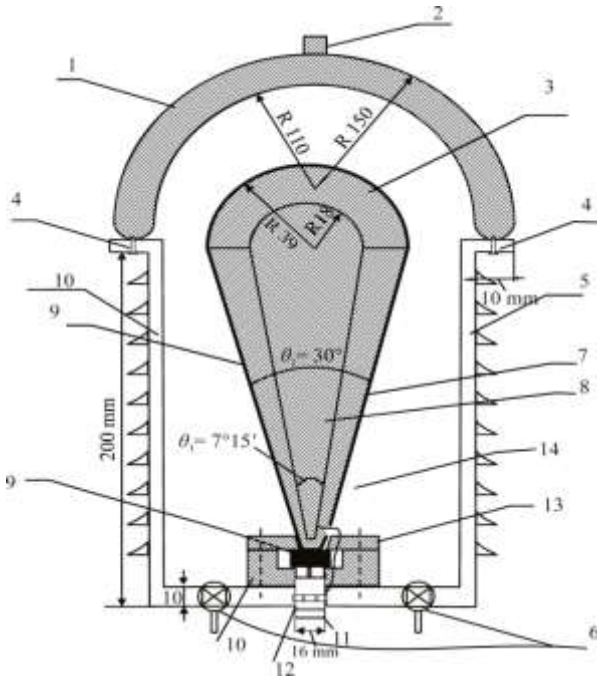

Sl. 6. Poprečni presek delitelja napona.
1– metal, 2– visokonaponski priključak, 3– metalni deo; 4– zaptivka, 5– plastična cev, 6– ventil za punjenje i pražnjenje, 7– dielektrik niskonaponskih kondenzatora, 8– metalni deo; 9– metalni deo, 10– plastični prsten, 11– fiksni deo BNC konektora, 12– priključna veza delitelja sa BNC konektorom (u tački između visoko i niskonaponske grane), 13– plastični prsten, 14– SF_6 gas 5 bar.

Niskonaponski kondenzator, kao što je rečeno, bio je izrađen kao paralelna veza 10 identičnih liskunskih kondenzatora. Liskunski kondenzatori su korišćeni zbog svoje frekventne karakteristike. Frekventna karakteristika liskuna je skoro konstantna s tim što ima uočljivo ulegnuće u oblasti delovanja polarizovanog prostornog naelektrisanja, slika 7. Razlog za to je lisnata struktura liskuna.

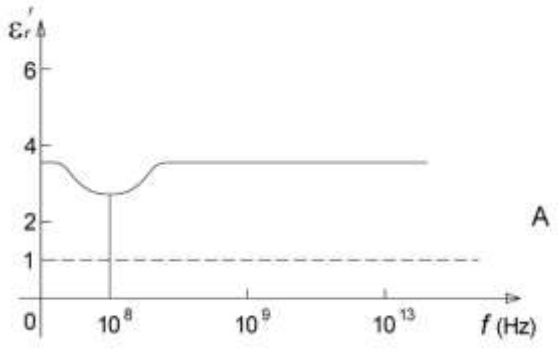

Sl. 7. Frekventna karakteristika liskunskog dielektrika korišćenih kondenzatora za izradu niskonaponskog kondenzatora.

Od velikog broja liskunskih kondenzatora za izradu niskonaponskih kondenzatora su izabirani oni sa identičnim vrednostima kapaciteta, tangensa ugla gubitaka, paralelne otpornosti i dielektrične konstante merena različitim naponima i frekvencijama. Od takvih kondenzatora je, standardizovanim postupkom, pravljen niskonaponski kondenzator delitelja. Ostatak kondenzatora, u grupama po 10, izloženi su kontrolisanom gama zračenju u laboratoriji za Zaštitu od zračenja i na jonizacionoj komori.

Zračenja su izvedena u kolimitiranom snopu proizvedenom od izvora zračenja Co-60. Izotop Co-60 izlaže se beta raspadu, nakon čega sledi fotonsko zračenje od 1,33 MeV i 1,17 MeV, sa verovatnoćom emisije blizu 1. Beta čestice koje se emituju tokom raspada ne doprinose dozi na mestu ispitivanja zbog zaštite izvora.

Referentne vrednosti su određene sa mernom nesigurnošću od 2.3 % (k = 2). Kondenzatori su ozračeni jedan po jedan, u laboratorijskim uslovima, na udaljenosti od 63.8 cm od izvora. Brzina doziranja na tački ispitivanja bila je 13.5 Gy/h, a vreme zračenja je odabrano tako da se sledeće doze isporuče u kondenzatore: 140 Gy, 170 Gy, 200 Gy, 220 Gy, 250 Gy, 280 Gy and 420.

Nakon ozračenja kondenzatora vršeno je merenje istih karakteristika kao i neozračenih kondenzatora. Zatim su i od ozračenih kondenzatora iste doze, pravljeni niskonaponski kondenzatori delitelja.

Nakon formiranja delitelja napona sa koncentrisanim visokonaponskim kondenzatorom pristupilo se testiranju delitelja kombinacijom numeričkog i eksperimentalnog postupka. Eksperimentalni postupak se sastojao od merenja odziva delitelja na Hevisajdov naponski impuls brzine porasta ns. Numerički postupak se sastojao primenom računarskih postupaka (EMTP ATP) na iste konfiguracije pod istim uslovima. Na slici 8 prikazana je fotografija sistema za snimanje odziva delitelja na primenjeni impuls. Na slici 9 prikazana je šema generatora impulsa za dobijanje Hevisajdovog step impulsa 5 ns [20-22].

Sl. 8. Fotografija sistema za snimanje odziva delitelja na pravougaoni impuls.

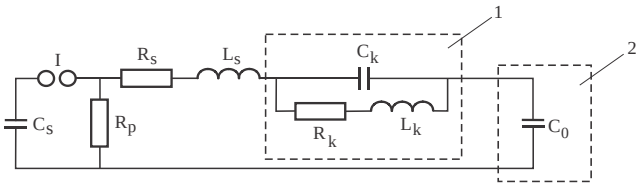

Sl. 9. Šema kompenzovanog generatora za dobijanje Hevisajdovog step impulsa porasta 5 ns; 1- kompenzaciona grana, 2- test objekat.

U toku eksperimenta merni uređaj se nalazio u zaštitnoj kabini zaštite preko 100 dB. Merni instrumenti u kabini su bili galvanski odvojeni od delitelja. Snimanja odziva delila su bila ponavljana po 100 puta. Na dobijenom statističkom uzorku vršena je detaljna statistička analiza [23,24]. Merna nesigurnost postupka je bila manja od 5 % [25-28].

IV. Rezultati i diskusija

Dejstvo primene doze na karakteristike liskunskih kondenzatora (a time i na niskonaponski kondenzator delila) prikazano je u tabeli 1. Iz tabele 1 se vidi da se kapacitet, tangens ugla gubitaka, impedansa i paralelna otpornost ekvivalentne šeme realnog kondenzatora poboljšavaju sa povećanjem doze zračenja. Ovaj neočekivani rezultat dolazi naročito do izražaja u slučaju frekventne karakteristike liskuna. Naime, efekat polarizacije prostornog naelektrisanja izražen u slučaju ozračenih kondenzatora znatno je manji nego u slučaju da kondenzator nije primio dozu zračenja. Ova promena frekventne karakteristike je jasno uočljiva ako se uporede frekventne karakteristike liskuna sa slike 7 (neozračeni uzorci) i sa slika 10a i 10b (ozračeni uzorci). Sa slika 10a i 10b se vidi da sa većom primljenom dozom zračenja više opada odstupanje frekventne konstante.

TABELA I

VREDNOSTI KAPACITETA, IMPEDANSE, INDEKSA GUBITAKA I PARALELNOG OTPORA POJEDINAČNIH NEOZRAČENIH I OZRAČENIH KONDENZATORA; ISPITNI NAPON U = 1 V; ISPITNA FREKVENCIJA F = 1000 HZ

Uzorak		**C7**		**C2**		**C4**		**C1**		**C6**	
Doza	Gy	0	**140**	0	**170**	0	**200**	0	**220**	0	**250**
Kapacitet	C (nF)	10.1930	11.7310	10.1720	11.6900	10.2060	11.7350	10.2080	11.7400	10.1700	12.2020
Impedansa	Z(kΩ)	15.6140	17.9480	15.6460	17.9900	15.5940	17.9470	15.5910	17.9500	15.6490	18.0550
Indeks gubitaka	tan δ	0.000698	0. 000665	0.000698	0. 000665	0.000698	0. 000665	0.000698	0.0006880	0.000698	0.000646
Paralelni otpor	R_0(MΩ)	22.3656	24.5300	22.4118	24.6442	22.3371	24.5741	22.3327	24.6400	22.4162	24.6400

Uzorak		**C5**		**C3**		**C10**		**C9**		**C8**	
Doza	Gy	0	**280**	0	**420**	0	**1400**	0	**14 000**	0	**42 000**
Kapacitet	C (nF)	10.1420	11.6600	10.1100	11.6150	10.1350	11.6570	10.1740	11.7500	10.1980	11.7370
Impedansa	Z(kΩ)	15.6930	18.0550	15.7420	18.1125	15.7030	18.0050	15.6430	17.9950	15.7420	17.9100
Indeks gubitaka	tan δ	0.000698	0. 000665	0.000698	0.000665	0.000175	0.000331	0.000698	0.000665	0.000698	0. 000665
Paralelni otpor	R_0(MΩ)	22.4781	24.7530	22.5492	24.7501	89.9744	49.4889	22.4070	24.6098	22.3546	24.5353

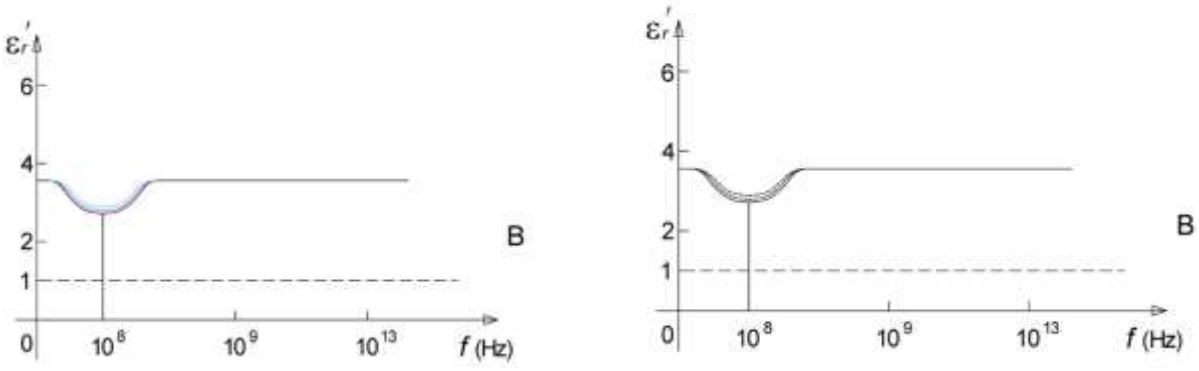

Sl. 10. Frekventna karakteristika liskunskog dielektrika korišćenih kondenzatora za izradu niskonaponskih kondenzatora; a) doza 420 Gy; b) doza 42 000 Gy.

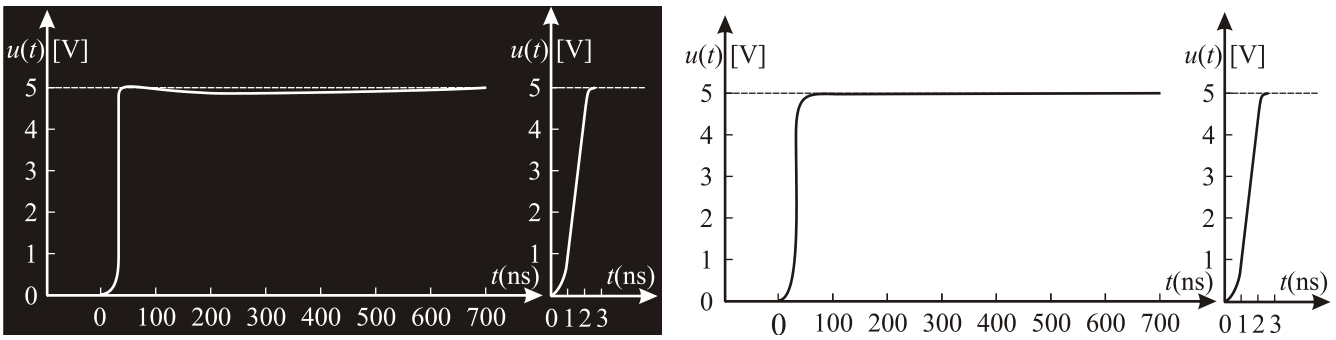

Sl. 11. Odziv kapacitivnih delitelja na pravougaoni impuls (izračunato).

Ovaj efekat, koji je izuzetno povoljan u slučaju liskunskih kondenzatora za niskonaponski kondenzator kapacitivnog delila posledica je strukture liskuna. Liskun je izrazito lisnate strukture. Kod liskuna van električnog polja dolazi do poklapanja pozitivnog i negativnog naelektrisanja usled Kulonovog efekta. To se dešava između svih slojeva liskuna. Međutim pod dejstvom električnog polja ta pozitivna i negativna naelektrisanja se razilaze i dolazi do polarizacije liskuna. Međutim pošto su listovi liskuna izuzetno tanki i mala deponovana energija gama zračenja može da ih pričvrsti (slepi) jedan uz drugi i time spreči njihovu polarizaciju. Po tom objašnjenju što je veća deponovana energija gama zračenja dolazi do veće homogenizacije liskunskog dielektrika što za posledicu ima smanjenje efekta prostorne polarizacije.

Na osnovu rezultata prikazanih u tabeli 1 može se zaključiti da parametri ispitivanih kondenzatora prate očekivane zavisnosti od primljene doze u skladu sa diagramima prikazanim na slikama 7 i 9. Iako se rezultati prikazani na slici 11 na prvi pogled čine istim pažljivom analizom se može ustanoviti da numerički eksperiment u oblasti srednjih frekvencija daje za preko 3 % veće vrednosti odzivne funkcije. To je posledica činjenice da numerički eksperiment koristi konstantnu vrednost realnog dela relativne dielektrične konstante. U slučaju neozračenih niskonaponskih kondenzatora ovo odstupanje je preko 9 %. U oblasti visokih frekvencija slaganje rezultata numeričkog i realnog eksperimenta je skoro 100 %. To se vidi na desnom delu slike 11.

V. ZAKLJUČAK

Dobijeni rezultati o uticaju gama zračenja na brzi, kompenzovani, kapacitivni delitelj sa liskunskim kondenzatorima u niskonaponskom kapacitetu pokazuju da primljena doza deluje u pravcu poboljšanja prenosnog odnosa delitelja. Međutim ni ovaj, prinudno pozitivan efekat, nije poželjan sa metrološke tačke gledišta. Naime svaki rezultat dobijen jednim mernim sistemom treba da bude reproduktivan. Međutim, u uslovima primene brzog delitelja napona koji se stalno nalazi u polju visokoenergetskog gama zračenja on, tako reći, kontinualno menja svoje prenosne karakteristike. To je nepoželjno pošto sprečava poređenje uzastopno dobijenih rezultata. Iz tog razloga, smatramo da ispitivanje treba nastaviti sa većim dozama zračenja da bi se utvrdilo da li uočeni efekat ulazi u saturaciju. Takođe smatramo da stabilnost prenosnog odnosa naponskog delitelja namenjenog primeni u ekperimentima nuklearne fuzije sa elektronskim injektovanjem energije u plazmu treba proširiti i na neutronsko polje. Naime, u ovom tipu eksperimenta javljaju se i neutroni velike srednje slobodne dužine puta koji mogu da interaguju sa niskonaponskim kondenzatorom delitelja. Naravno dobijeni rezultat je važan, i primenjiv, za delila napona koja ne rade u polju gama zračenja pošto nepovratno popravlja njihove prenosne karakteristike.

LITERATURA

[1] Osmokrovic, P., Arsic, N., Kartalovic, N., Triggered three-electrode spark gaps, (1995) Digest of Technical Papers-IEEE International Pulsed Power Conference, 2, pp. 822-827.

[2] A. Schwab, Hochspannungsmeß-technik, Springer – Verlag, Berlin, Germany, 1981.

[3] International Atomic Energy Agency, Calibration of Radiation Protection Monitoring Instruments, IAEA Safety Reports Series No.16, Vienna, (2000).

[4] Vereb, L., Osmokrović, P., Vujisić, M., Lazarević, Z., Kartalović, N., Effect of insulation construction bending on stator winding failure, (2007) IEEE Transactions on Dielectrics and Electrical Insulation, 14 (5), pp. 1302-1307.

[5] BIPM, IEC, IFCC, ISO, IUPAC, IUPAP and OIML, The International Vocabulary of Basic and General Terms in Metrology, International Organization for Standardization, Geneva (1993).

[6] P. Osmokrović, N. Arsić, Z. Lazarević and Z. Kusić „Numerical and experimental design of three – electrode spark gap for synthetic test circuits“, IEEE Transactions on Power Delivery, Vol. 9, No. 3, pp. 1444 – 1450, July 1994.

[7] P. Osmokrović, D. Filipović, M. Pešić and Z. Lazarević, „Transient electric field measurement in the liquid dielectrics using computerized laser tomography“, IEEE Transactions on Instrumentation and Measurement, Vol. 56, No. 6, pp. 2538 – 2546, December 2007.

[8] P. Osmokrović, I. Milovanović, M. Vujisić, K. Stanković, R. Radosavljević, „Experimental measurements of very fast transient voltages based on an electro-optic effect“, International Journal of Electrical Power & Energy Systems, Vol. 43, No. 1, pp. 408 – 417, 2012.

[9] Kartalović, N.M., Jokanović, B.M., Bebić, M.Z., Lazarević, D.R., Degradation of stator insulation of high-voltage asynchronous machines in gamma and neutron radiation field, (2019) Nuclear Technology and Radiation Protection, 34 (3), pp. 264-271.

[10] N. Arsić, P. Osmokrović and I. Milovanović, ”The influence of the Low¬Voltage capacitor dielectric material on the capacitive probe response in the nanosecond range“, Digest of Technical Papers ¬ 2005 IEEE Pulsed Power Conference, Monterey, CA, United States, pp. 726¬729, 13-17. June 2005.

[11] Dolićanin, E.Ć., Fetahović, I.S., Monte Carlo optimization of redundancy of nanotechnology computer memories in the conditions of background radiation, (2018) Nuclear Technology and Radiation Protection, 33 (2), pp. 208-216.

[12] Trifunović-Dragišić, V.Z., Stanković, M.D., Brajović, D.V., Kartalović, N.M., Estimation of the lifetime of solar cells in real conditions using

accelerated aging under the influence of neutron and gamma radiation, (2019) Nuclear Technology and Radiation Protection, 34 (3), pp. 256-263.
[13] Osmokrovic, P., Stojanovic, M., Loncar, B., Kartalovic, N., Krivokapic, I., Radioactive resistance of elements for over-voltage protection of low-voltage systems, (1998) Nuclear Instruments and Methods in Physics Research, Section B: Beam Interactions with Materials and Atoms, 140 (1-2), pp. 143-151.
[14] A. Kuchler, Hochspannungstechnik, Springer, Berlin, 2009.
[15] G. Yue, W. Liu, W. Chen, Y. Guan, Z. Li and H. Wang, "Measurement methods of very fast transient overvoltage in gas insulated switchgear with complete process", Proceedings of the Chinese Society of Electrical Engineering, Vol. 31, pp. 18¬27, 2011.
[16] P. Osmokrović, D. Petković, O. Marković, N. Kartalović, Đ. Vukić: Measuring System for Fast Transient Monitoring in Gas – Insulated Substations, ETEP, 1997, Vol. 24, No. 6, pp. 165-172.
[17] IEC Publication Nr. 60060-1: High – voltage test techniques – Part 1: General definitions and test requirements, IEC 1989, Genf.
[18] P. Osmokrović, D. Petković and O. Marković, "Measuring probe for fast transients monitoring in gas - insulated substations", ETEP/IEEE Trans. Instrum. Meas., Vol. 46, pp. 36-45, 1997.
[19] Obrenović, M.D., Pejović, M.M., Lazarević, D.R., Kartalović, N.M., The effects induced by the gamma-ray responsible for the threshold voltage shift of commercial p-channel power VDMOSFET, (2018) Nuclear Technology and Radiation Protection, 33 (1), pp. 81-86.
[20] HAEFELY Documentation: Impulse Current Test Sistem, Type SSGA 30-200 kA, Basel, 2001.
[21] P. Osmokrović, G. Ilić, K. Stanković, Ć. Dolićanin, M. Vujisić: Determination of Pulse Tolerable Voltage in Gas-Insulated Systemy, Japanese Journal of Applied Physics Vol. 47 (2008), pp. 8928-8934.
[22] M. Stojkanović, G. Djukić, K. Stanković, M. Vujisić and P. Osmokrović, "Design Deployment and verification of the capacitive voltage divider for measuring fast transient occurrences in the nanosecond range", Int. J. Elec Power, Vol. 43, pp. 1479-1486, 2012.
[23] Čaršimamović, A.S., Mujezinović, A.Z., Bajramović, Z.F., Turković, I.M., Košarac, M.P., Low frequency electric field radiation level around high-voltage transmission lines and impact of increased voltage values on the corona onset voltage gradient, (2018) Nuclear Technology and Radiation Protection, 33 (2), pp. 201-207.
[24] BIPM, IEC, IFCC, ISO, IUPAC, IUPAP and OIML, Guide to the Expression of Uncertainty in Measurement, International Organization for Standardization, Geneva (1995).
[25] Jusić, A., Bajramović, Z., Turković, I., Mujezinović, A., Osmokroć, P.V., Synergy of radioactive 241Am and the effect of hollow cathode in optimizing gas-insulated surge arresters characteristics, (2018) Nuclear Technology and Radiation Protection, 33 (3), pp. 260-267.
[26] Jeftenić, I., Kartalović, N., Brajović, D., Lončar, B., Aging of stator coil interconductor insulation of high voltage asynchronous motor, (2018) IEEE Transactions on Dielectrics and Electrical Insulation, 25 (1), pp. 352-359.
[27] Perazić, L.S., Belić, Č.I., Arbutina, D.B., Application of an electronegative gas as a third component of the working gas in the Geiger-Mueller counter, (2018) Nuclear Technology and Radiation Protection, 33 (3), pp. 268-274.
[28] Obrenović, M.D., Janićijević, A.J., Arbutina, D.S., Statistical review of the insulation capacity of the geiger-mueller counter, (2018) Nuclear Technology and Radiation Protection, 33 (4), pp. 369-374.

ABSTRACT

The effect of gamma radiation on the reliable measurement of single voltage pulses of electron beam injectors into plasma during fusion experiments is considered in the manuscript. For this purpose, a 10 GHz fast voltage divider was constructed. The high-voltage capacitor was a gas condenser, and the low-voltage capacitor was a parallel connection of 10 mica capacitors. It turned out that the received radiation dose corrects the transmission ratio since it aligns the frequency characteristic of the mica in the area of spatial charge. This phenomenon has been explained from both a positive and a negative aspect with an effect on concrete application. The need for further research on this problem was also pointed out in order to establish a saturation dose to obtain a constant frequency characteristic of the mica. The interest in the fast-divider behavior in the neutron field is also highlighted.

Influence of gamma radiation on the measurement uncertainty of a fast, compensated capacitive divider

Nenad Kartalović, Koviljka Stanković, Dušan Nikezić, Tomislav Stojić, Uzahir Ramadani i Uroš Kovačević

Utilization of Waste-Based Geopolimers for Radionuclide Immobilization – A Review

Slavko Dimović, Ivana Jelić and Marija Šljivić-Ivanović

Abstract — **The aim of this article is to review the utilization of waste components for radionuclides immobilization by geopolymerization. The geopolymers represent a wide range of alkaline-activated aluminosilicates. Synthesis of geopolymers from waste provides less raw material consumption and addresses issues regarding the disposal of waste. Fly ash, red mud, construction and demolition waste, or slags are the most utilized waste types. The advantage of these waste materials represents the possibility of utilization of any aluminosilicate-containing waste that could be dissolved in an alkaline solution to produce a matrix for radionuclide immobilization. Despite many publications and investigations concerning the usage of waste components in geopolymerization, the utilization of waste-based geopolymers in the disposal of radionuclides has not yet been developed enough.**

Keywords — **radionuclides; waste; geopolymers; recycle; reuse.**

I. Introduction

The fast technological progress led to a realization of a large amount of waste to the environment, increased non-renewable natural resource extraction, and energy consumption [1-3]. The safe disposal of different kinds of waste and industrial by-products has become a key concern worldwide [4]. Problems arising from a substantial amount of waste have gained great social and environmental importance [1]. The investigation of waste reusing to produce new products has been expansively carried out [5-6].

The term geopolymer and its description as cement-free green cementitious material were introduced in the late 70s [7]. In past years, geopolymerization technology has been shown advantages in reusing various types of waste for the production of the new materials for many purposes. These so-called inorganic polymers [7], have been proposed for the utilization of solid aluminosilicate waste and the development of new materials [8]. Geopolymers have gained attention primarily due to the ease of synthesis with little or zero-emission of greenhouse gases [9]. Hence, the utilization of geopolymers could show many advantages such as usage of low-cost waste materials in production (e.g. slags, fly ash, various clays, and even agricultural wastes), saving natural resources, ambient temperature production, and high compressive and flexural strengths, in particular as compared to cement [7-8]. All these characteristics are placing them in a category of new eco-friendly and sustainable materials.

Geopolymers are structurally and chemically comparable to rocks and are synthesized by condensation mechanisms similar to organic polymers [7]. The geopolymerization represents a process comprising of the dissolution of aluminosilicate solids in a strongly alkaline medium followed by condensation of free alumina-silica oligomers to form a tetrahedral polymeric structure [7,10]. During this process, activated aluminosilicate is dissolved in an alkaline solution to form free $SiO4^{-}$ and $AlO4^{-}$ ions charge-balanced by hydrated alkali cations. Ions are tetrahedrally coordinated, forming amorphous or semi-crystalline oligomers. Finally, geopolymer gel is created by polymerization and hardening of oligomers [11] (Fig.1).

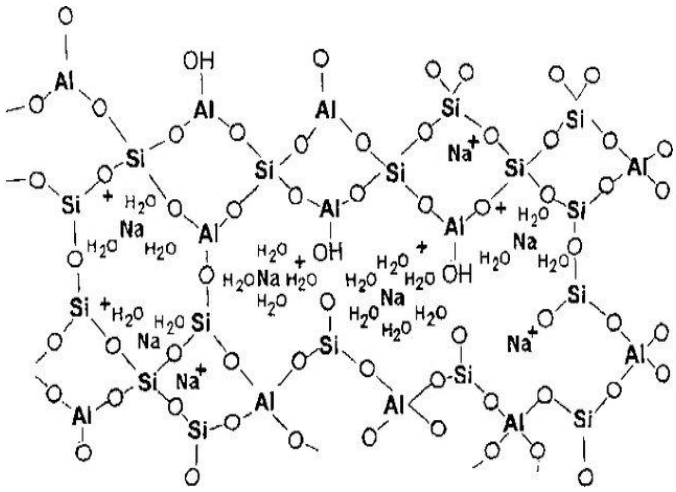

Fig. 1. Model of geopolymer structure [12]

The empirical formula of geopolymer could be shown as [7,12-13]:

$$M_n[-(SiO_2)_z-AlO_2^-]_n \cdot\cdot\ wH_2O$$

where:
M – alkaline or alkaline-earth cation;
n – degree of poly-condensation;
z – number, generally <3 for three-dimensional structure;
w – number of crystalline water molecules.

Slavko Dimović – Vinca Institute of Nuclear Sciences, University of Belgrade, P.O. Box 522, 11000 Belgrade, Serbia (e-mail: sdimovic@vin.bg.ac.rs).

Ivana Jelić – Vinca Institute of Nuclear Sciences, University of Belgrade, P.O. Box 522, 11000 Belgrade, Serbia (e-mail: ivana.jelic@vin.bg.ac.rs).

Marija Šljivić-Ivanović – Vinca Institute of Nuclear Sciences, University of Belgrade, P.O. Box 522, 11000 Belgrade, Serbia (e-mail: marijasljivic@vin.bg.ac.rs).

Compared to conventional construction materials, e.g. concrete, the synthesized geopolymers show adequate physicomechanical properties, such as high strengths [14]. Likewise, geopolymers are fire resistant up to 1400°C, heat, and acid-resistant materials. They exhibit high early compressive strength, low porosity, and freeze-thaw resistance, e.g. long-term durability [7-8,12]. However, their most important advantage is that, depending on their design, they acquire properties tailored to the needs of the end-user [8].

The aim of this article is to review the utilization of waste components for radionuclides immobilization by geopolymerization. However, the immobilization of radionuclides in the waste-based geopolymers was rarely investigated, according to available data, unlike very comprehensive research on heavy metals [15]. Geopolymerization technology has been proposed to stabilize and solidify a simulated residue containing hazardous metals [16]. Although, a few studies from the past several years have pointed out that radionuclides could be immobilized in the geopolymer matrix. Also, the results for some heavy metals immobilization by geopolymers could be used for these purposes.

II. Radionuclide Immobilization Practice

The usual procedures for the immobilization of radioactive waste are technological operations of converting these materials into stable insoluble forms using matrix materials (solidification). Standard matrices for immobilization of radioactive waste are cement, mortar, concrete, bitumen, polymers (e.g. plastics) or borosilicate glass, etc. [17-18]. Conditioning processes such as cementation and vitrification are often used to convert waste into a stable solid form insoluble and prevent dispersion to the surrounding environment.

A systematic approach typically incorporates the identification of a suitable matrix material that will ensure the stability of the radioactive materials for the period necessary. The type of waste being conditioned determines the choice of matrix material and packaging. Conditioning of radioactive waste implies operations of transformation into forms suitable for later manipulation (handling, transport, temporary storage, and permanent disposal).

Also, investigation of the sorption process in order to prevent the interaction of radionuclides with living tissue and their accumulation (since these ions are not biodegradable like most organic substances [19], while radionuclides emit extremely dangerous radioactive radiation [20]), as well as monitoring the process of their migration in the environment and finding technological innovations for their immobilization is currently expanding. A large number of researches are based on finding sorbents of the highest efficiency, i.e. sorption capacity, and the lowest possible production costs. Due to the topicality, numerous studies have examined various sorbent materials that are readily available locally and whose economic viability can justify their widespread usage.

Sorption of radionuclides from liquid radioactive waste (LRW), i.e. from a suspension or solution, onto waste materials is based on finding the sorbents with as much higher sorption capacity while reducing the cost of their production [21]. For example, the immobilization of LRW (and heavy metals) using stony C&DW or its components has been increasingly investigated over the last few years [21], due to the similarity of the cement matrix usually used for radionuclide immobilization. Various types of cementitious material, namely concrete and facade material, clay-based materials such as bricks, ceramic and roof tiles, as well as waste asphalt, were consistently investigated [22-24].

Studies have shown that the immobilization of ions in geopolymer matrixes also includes the sorption processes. Sorption on a synthesized geopolymer could be studied as a function of the geopolymer dosage, ions initial concentration, contact time, pH, and temperature [25-27].

III. Radionuclide Immobilization by Waste-based Geopolymers

The very high costs of immobilization, temporary storage, and final disposal of LRW and wastewater heavy metals treatment, stimulate research into the development of cost-effective materials, which during production or after usage represent final waste [28]. Particular attention should also be paid to European legislation that encourages the development of a “circular economy”, which implies the efficient use of materials [29]. However, the thermal stability and acid corrosion resistance of cement-based materials are relatively low [30]. Moreover, the utilization of other materials, such as glass and resin, is limited by their high cost and complex preparation [31]. Because of its excellent mechanical performance, such as compressive strength, acid/alkaline resistance, and heat resistance, geopolymers have become ideal materials for solidifying toxic waste [15].

In recent studies, the waste aluminosilicates were used to synthesize different geopolymers as heavy metal, as well as radionuclides immobilizing matrixes. The raw materials mainly used in geopolymerization are clays or pozzolanic materials such as kaolin, calcined kaolin, different fly ashes, and blast furnace slags partially dissolve in the alkali solution [16]. Conversion of fly ash to an amorphous aluminosilicate sorbent, i.e. geopolymer has been investigated under different conditions and was paid great attention as a potential material for removal of Ni(II), Pb(II), Cu(II), and radionuclides: ^{137}Cs and ^{90}Sr [32]. The geopolymer testing also included key radionuclides such as Tc, I, Sr, and Cs [33-39], as well as ^{152}Eu, ^{60}Co, and ^{59}Fe isotopes [40], which dominate the risk to the environment. For example, 20 – 30 years after the nuclear reactor shutdown, taking into account fission and corrosion products, the most abundant radionuclides in contamination residues generally include ^{63}Ni, ^{137}Cs, ^{60}Co, and ^{90}Sr [41]. In solidification systems made by geopolymerization, geopolymers exhibit different immobilization efficiencies toward different ions, and the mechanisms vary. Zhang et al. [26] reported that Pb(II) could be immobilized in geopolymers

more effectively compared to Cd(II) and Cr(VI). Wang et al. [27] determined that solidification of Pb(II), Cd(II), Mn(II), and Cr(III) in a fly ash-based geopolymer occurs by exchange with ions including Na(I) and Ca(II). However, El-Eswed et al. [33] argued that rather than ion exchange, ions including Pb(II), Cd(II), Cu(II), Th(IV), and U(VI) are immobilized by forming chemical bonds between Si–O^- and Al–O^-. Xu et al. [34] and Peng et al. [35] compared the immobilization efficiency of Sr(II) and metakaolin geopolymer with cement and found that Sr(II) showed a higher leaching resistance. They concluded that the geopolymer matrix appeared more compact and dense, which encapsulated Sr more tightly. Among the studies on Co(II) immobilizing, metakaolin is generally used as the starting material. Kara et al. [42] studied the performance of the metakaolin geopolymer for Co(II) removal, but the immobilization rate for Co(II) was lower than for Mn(II). El-Naggar [43] improved the immobilization effect of 60Co by adding blast furnace slag to Egyptian kaolinite and reported that this geopolymer's compressive strength was significantly enhanced. In recent research, Q. Yu et al. [44] compared the performance of immobilizing Co with the Mn slag-based geopolymer and an ordinary metakaolin-based geopolymer. The results strongly suggested that divalent Co was oxidized to trivalent Co in the Mn slag-based geopolymer matrix, resulting in enhanced Co solidification capacity compared to a metakaolin-based geopolymer. The results in this study indicate that the Mn slag-based geopolymer's oxidation environment played an important role in Co immobilization [44].

Although geopolymers are considered as promising matrixes for waste solidification, the effects of the Si/Al molar ratio of geopolymer on the immobilization efficiencies for metal ions have not been fully studied and understood. Q. Tian et al. [37], were synthesized and investigated geopolymers with different Si/Al ratios from coal fly ash and silica fume. Sorption tests were conducted to evaluate their immobilization efficiencies for Cs^+. The results indicated that a geopolymer with a low Si/Al ratio could have a better immobilization performance for Cs^+ than that with a high Si/Al ratio. A high Si/Al ratio could contribute to a more compact structure of geopolymer and better sorption process [37].

Likewise, in novel investigations, a geopolymer was applied to convert ion exchange resins contaminated with radionuclides into a solid waste form. It was found that a geopolymer has superior properties to enable the encapsulation of spent resins [45-46]. However, there is limited understanding of the chemical interactions between encapsulated spent ion-exchangers, used for decontaminating wastewater, and aluminosilicate matrix. This fact makes it difficult to predict the long-term stability of the waste form [46].

Radionuclides Cs and Sr are two of the most difficult radionuclides to immobilize and are therefore suitable elements to study in assessing geopolymers as matrices for immobilization of radioactive wastes [39,47].

IV. Conclusion

With the increasing depletion of natural raw materials, their sustainable usage is an important topic for consideration. Therefore, the development of sustainable and low carbon footprint materials is an important task for the future. Thus, waste-based geopolymers have found a possible application in the immobilization of radionuclides. This paper aims to review so far knowledge related to the utilization of waste-based geopolymers in radionuclides immobilization. All results from cited studies suggest that waste-based geopolymers represent promising matrix materials for the solidification of radioactive wastes, but more precise investigations are needed.

Acknowledgments

This work was supported by the Ministry of Education, Science and Technological Development of the Republic of Serbia.

References

[1] C.S. Vieira, P.M. Pereira, "Use of recycled construction and demolition materials in geotechnical applications: A review", *Res. Resour. Conserv. Recycl*., vol. 103, pp. 192-204, 2015.

[2] C. Zou, Q. Zhao, G. Zhang, B. Xiong, "*Energy revolution: from a fossil energy era to a new energy era*", Nat. Gas Ind. B, vol. 1, pp. 1-11, 2016.

[3] O. Blanchard, "Energy consumption and modes of industrialization: Four developing countries", *En. Policy*, vol. 20, pp. 1174-1185, 1992.

[4] S.S. Amritphale, P. Bhardwaj, R. Gupta, "Advanced Geopolymerization Technology", in *Geopolymer Science and Applications*, ch. 1, pp. 1-11, London, UK: Intech Open, 2019.

[5] European Commission, Waste Framework Directive 2008/98/EC, Off. Journal of the European Union, L 312, https://eur-lex.europa.eu/legal-content/EN/TXT/PDF/?uri=CELEX: 32008L0098& from=EN

[6] Environment Action Programme EU 2013, Living well, within the limits of our planet, https://eur-lex.europa.eu/legal-content/EN/TXT/?uri=CELEX:32013D1 386

[7] J. Davidovits, "Geopolymers", *J. Thermal Anal.*, vol. 37, pp. 1633-1656, August, 1991.

[8] J.L. Provis, "Geopolymers and other alkali activated materials: why, how, and what?", *Mater.Struct.*, vol. 47, pp. 11-25, January, 2014.

[9] A. Noorul, M. Faisal, K. Muhammad, S. Gul, Synthesis and characterization of geopolymer from bagasse bottom ash, waste of sugar industries and naturally available China clay. *J. Clean. Prod.*, vol. 129, pp. 491-495, 2016.

[10] J.L. Provis, A. Palomo, C. Shi, "Advances in understanding alkali-activated materials", *Cem. Concr. Res.*, vol. 78, pp. 110-125, 2015.

[11] P. Duxson, A. Fernández-Jiménez, J.L. Provis, G.C. Lukey, A. Palomo, J.S.J. van Deventer. "Geopolymer Technology: The Current State of the Art", *J. Mater. Sci*., vol. 42, no. 9, pp. 2917-2933, 2007.

[12] J. Davidovits, *Geopolymers-Inorganic polymeric new material*, Reprint of Journal of Thermal Analyses (1991), Saint-Quentin, France, Institut Géopolymère, 1997.

[13] Y. Hu, S. Liang, J. Yang, Y. Chen, N. Ye, Y. Ke, S. Tao, K. Xiao, J. Hu, H. Hou, W. Fan, S. Zhu, Y. Zhang, B. Xiao, "Role of Fe species in geopolymer synthesized from alkali-thermal pretreated Fe-rich Bayer red mud", *Constr. Build. Mater*., vol. 200, pp. 398-407, 2019.

[14] J.S.J. Van Deventer, J.L. Provis, P. Duxson, G.C. Lukey, "Reaction mechanisms in the geopolymeric conversion of inorganic waste to useful products", *J. Hazard. Mater*., vol. 139 pp. 506-513, 2007.

[15] T. Cheng, M. Lee, M. Ko, T. Ueng, S. Yang, S. The heavy metal adsorption characteristics on metakaolin-based geopolymer. *Appl. Clay Sci*., vol. 56, pp. 90-96, 2012.

[16] C. Fernández-Pereira, Y. Luna-Galiano, M. Pérez-Clemente, C. Leiva, F. Arroyo, R. Villegas, L.F. Vilches, Immobilization of heavy metals (Cd, Ni or Pb) using aluminate geopolymers, *Mater. Lett.*, vol. 227, pp. 184-186, 2018.

[17] M. I., Ojovan, W. E., Lee, *An Introduction to Nuclear Waste Immobilization*, Second edition. Elsevier, 2014.
[18] S., Stefanovsky, S., Yudintsev, R., Giere, G., Lumpkin, *Nuclear waste forms*, The Geological Society of London, London, UK, 2004.
[19] D. Nies, S. Silver, *Molecular Microbiology of Heavy Metals*. Springer. Berlin, Germany, 2007.
[20] C. Grupen, M. Rodgers, *Radioactivity and Radiation*, Springer, Berlin, Germany, 2016.
[21] I. Jelic, M. Sljivic-Ivanovic, S. Dimovic, D. Antonijevic, M. Jovic, M. Mirkovic, I. Smiciklas, The Applicability of Construction and Demolition Waste Components for Radionuclide Sorption, *J. Clean. Prod*., vol. 171, pp. 322-332, 2018.
[22] I. Jelic, M. Sljivic-Ivanovic, S. Dimovic, D. Antonijevic, M. Jovic, R. Serovic, I. Smiciklas, Utilization of Waste Ceramics and Roof Tiles for Radionuclide Sorption, Process Saf Environ, 105, pp. 348-360, 2016.
[23] M. Sljivic-Ivanovic, I. Jelic, A. Loncar, D. Nikezic, S. Dimovic, B. Loncar, The application of experimental design methodology for the investigation of liquid radioactive waste treatment. Nucl Technol Radiat, vol. 32, no. 3, pp. 281-287, 2017.
[24] M. Sljivic-Ivanovic, I. Jelic, S. Dimovic, D. Antonijevic, M. Jovic, A. Mrakovic, I. Smiciklas, Exploring innovative solutions for aged concrete utilization: treatment of liquid radioactive waste, Clean Technol Envir, vol. 20, no. 6, pp. 1343-1354, 2018.
[25] K. Al-Zboona, M. S. Al-Harahshehb, F.B. Hani, Fly ash-based geopolymer for Pb removal from aqueous solution, *J. Hazard. Mater*., vol. 188, pp. 414-421, 2011.
[26] J. Zhang, J.L. Provis, D. Feng, J.S. van Deventer, Geopolymers for immobilization of Cr(VII), Cd(II), and Pb(II). *J. Hazard Mater*., vol. 157, no. (2-3), pp. 587-598, 2008.
[27] Y. Wang, F. Han, J. Mu, Solidification/stabilization mechanism of Pb(II), Cd(II), Mn(II) and Cr(III) in fly ash based geopolymers, *Constr. Build. Mater*., vol. 30, no. 160, pp. 818-827, 2018.
[28] F. Fu, Q. Wang, Removal of heavy metal ions from wastewaters: A review, *J. Environ. Manage*., vol. 92, pp. 407-418, 2011.
[29] M. Grace, E. Clifford, M. Healy, The potential for the use of waste products from a variety of sectors in water treatment processes, *J. Clean. Prod*., vol. 137, pp. 788-802, 2016.
[30] R. Malviya, R. Chaudhary, Factors affecting hazardous waste solidification/stabilization: A review. *J. Hazard Mater*., vol. 137, no. 1, pp. 267-276, 2006.
[31] J. Li, J., Wang, Advances in cement solidification technology for waste radioactive ion exchange resins: A review. J. Hazard Mater., vol. 135, no. (1-3), pp. 443-448, 2006.
[32] M. Ahmaruzzaman, A review on the utilization of fly ash, *Prog. Energy Combust. Sci.*, vol. 36, no. 3, pp. 327-363, 2010.
[33] B.I. El-Eswed, O.M. Aldagag, F.I. Khalili, Efficiency and mechanism of stabilization/solidification of Pb(II), Cd(II), Cu(II), Th(IV) and U(VI) in metakaolin based geopolymers, *Appl. Clay Sci*., vol. 140, pp. 148-156, 2017.
[34] Z. Xu, Z. Jiang, D. Wu, X. Peng, Y. Xu, N. Li, Y. Qi, P. Li, Immobilization of strontium-loaded zeolite A by metakaolin based-geopolymer. Ceram. Int., vol. 43, no. 5, pp. 4434-4439, 2017.
[35] X. Peng, Y. Xu, Z. Xu, D. Wu, D. Li, Effect of simulated radionuclide strontium on geopolymerization process, *Procedia Environ. Sci*., vol. 31, pp. 325-329, 2016.
[36] N. Deng, H. An, H. Cui, Y. Pan, B. Wang, L. Mao, J. Zhai, Effects of gamma-ray irradiation on leaching of simulated 133Cs+ radionuclides from geopolymer wasteforms, *J. Nucl. Mater*., vol. 459, pp. 270–275, 2015.
[37] Q. Tian, S. Nakama, K. Sasaki, Immobilization of cesium in fly ash-silica fume based geopolymers with different Si/Al molar ratios, Science of the Total Environment, vol. 687, pp. 1127–1137, 2019.
[38] X. Liu, Yi D. Lu, X. Lu, Immobilization of Simulated Radionuclide ^{90}Sr by Fly Ash-Slag-Metakaolin–Based Geopolymer, *Nucl Technol*, vol. 198, no. 1, pp. 64-69, 2017.
[39] B. Walkleya, X. Kea, O.H. Hussein, S.A. Bernal, J.L. Provis, Incorporation of strontium and calcium in geopolymer gels, *J. Hazard Mater*, vol. 382, no. 121015, 2020.
[40] T. Hanzlicek, M. Steinerova, P. Straka, Radioactive Metal Isotopes Stabilized in a Geopolymer Matrix: Determination of a Leaching Extract by a Radiotracer Method, J. Am. Ceram. Soc., vol. 89, no. 11, pp. 3541-3543, 2006.
[41] International Atomic Energy Agency (IAEA), Radiological Characterization of Shut Down Nuclear Reactors for Decommissioning Purposes, Technical Reports Series No. 389, Vienna, 1998.
[42] I. Kara, D. Tunc, F. Sayin, S.T. Akar, Study on the performance of metakaolin based geopolymer for Mn(II) and Co(II) removal, *Appl. Clay Sci.*, vol. 161, pp. 184-193, 2018.
[43] M.R. El-Naggar, Applicability of alkali activated slag-seeded Egyptian Sinai kaolin for the immobilization of 60Co radionuclide. *J. Nucl. Mater.*, vol. 447, pp. 15-21, 2014.
[44] Q. Yu, S. Li, H. Li, X. Chai, X. Bi, J. Liu, T. Ohnuki, Synthesis and characterization of Mn-slag based geopolymer for immobilization of Co, *J. Clean. Prod*, vol. 234, 97-104, 2019.
[45] W.H. Lee, T.W. Cheng, Y.C. Ding, K.L. Lin, S.W. Tsao, C.P. Huang, Geopolymer technology for the solidification of simulated ion exchange resins with radionuclides, *J Environ Manage*, vol. 235, pp. 19-27, 2019.
[46] X. Ke, S.A. Bernal, T. Sato, J.L. Provis, Alkali aluminosilicate geopolymers as binders to encapsulate strontium-selective titanate ion-exchangers, *Dalton Trans*., vol. 48, pp. 12116-12126, 2019.
[47] N. Vandevenne, R.I. Iacobescu, R. Carleer, P. Samyn, J. D'Haen, Y. Pontikes, S. Schreurs, W. Schroeyers, Alkali-activated materials for radionuclide immobilisation and the effect of precursor composition on Cs/Sr retention, *J. Nucl. Mater.*, vol. 510, pp. 575-584, 2018.

APSTRAKT

Cilj ovog rada je pregled upotrebe otpadnih komponenti za imobilizaciju radionuklida geopolimerizacijom. Geopolimeri predstavljaju širok spektar aluminosilikata koji se aktiviraju u alkalnoj sredini. Sinteza geopolimera iz otpada ne samo da omogućava manju potrošnju sirovina, već se bavi i pitanje odlaganja otpada. Leteći pepeo, crveni mulj, građevinski otpad i šljaka su najčešće korišćene vrste otpada. Prednost ovih otpadnih materijala predstavlja mogućnost upotrebe bilo kog aluminosilikatnog otpada koji može da se rastvori u alkalnom rastvoru kako bi se proizveo matriks za imobilizaciju radionuklida. Uprkos mnogim publikacijama i istraživanjima u vezi korišćenja otpadnih komponenti u geopolimerizaciji, upotreba geopolimera na bazi otpada pri odlaganju radionuklida još uvek nije razvijena.

Upotreba geopolimera na bazi otpada za imobilizaciju radionuklida - Pregled

Slavko Dimović, Ivana Jelić i Marija Šljivić-Ivanović

Establishing the RQR radiation qualities in the Secondary Standard Dosimetry Laboratory

Nikola Kržanović, Miloš Živanović, Olivera Ciraj-Bjelac, Predrag Božović, Andrea Kojić

***Abstract*—Quality assurance in the area of diagnostic radiology is performed by examining X-ray output parameters under medical exposure irradiation conditions using calibrated dosimetry equipment. The diagnostic radiology dosimeters are calibrated in reference radiation fields established according to IEC 61267 international standard. In practice, radiation qualities are defined by the X-ray tube voltage and the half-value layer and homogeneity coefficient. Comparison of these parameters with the recommendations of the standard can be used for incident photon spectrum characterization and modification by improving the added filtration for each radiation quality, thus acquiring the desired half-value layer for the given X-ray tube voltage. For most of the diagnostic radiology radiation qualities available at the Secondary Standard Dosimetry Laboratory a deviation of the first half-value layer less than ±3% was achieved, with an exception of one radiation quality where a correction would be required.**

***Index Terms*—Diagnostic radiology; Half-value layer; Homogeneity coefficient, X-ray.**

I. Introduction

THE medical imaging procedures in diagnostic radiology utilize radiation fields consisting of a wide range of different X-ray photon energies. In order to improve the quality of diagnostic procedures in hospitals, periodic quality assurance (QA) testing of X-ray generators is performed. The dosimetry equipment used for these measurements should be calibrated in a Standard Dosimetry Laboratory, ensuring the traceability to the primary standard for kerma free-in-air. For the dosimetry equipment calibration purposes, radiation fields with specific parameters and known spectra are defined as radiation qualities. Full characterization of the radiation qualities can be performed by measuring the photon fluence spectra. Due to the complexity of the X-ray spectrometry measurements, in practice these radiation qualities are defined with X-ray tube voltage and the half-value layer (HVL) [1]. For the equipment calibration in the direct beam in diagnostic radiology, RQR (Radiation Qualities in Radiation beams emerging from the X-ray source assembly) series radiation qualities are used, as defined in IEC 61267 [1] [2].

By establishing the radiation qualities considering the recommendations of the international standard, calibrations of the dosimetry equipment can be performed in radiation fields which are closely related to the radiation fields present under the medical exposure conditions. For specific diagnostic radiology applications such as mammography and computerized tomography, IEC 61267 defined radiation qualities RQR-M and RQT are used, respectively [2].

On the other hand, non-standard radiation qualities might be more appropriate for specific fluoroscopy applications, essentially those in interventional radiology and interventional cardiology procedures. Therefore, in order to improve the calibration procedures of the QA dosimeters, under the framework of the VERIDIC project, a series of non-standard radiation qualities, which closely describe medical exposure radiation fields in interventional radiology and interventional cardiology procedures, has been developed [3].

Due to the diagnostic radiation quality beam hardening it is not sufficient to describe the beam by solely determining the first HVL, therefore the determination of the first and second HVL is required. Considering the exponential law of attenuation of the primary beam, the first and second HVL are defined as:

$$HVL_1 = d_{1/2} = \frac{\ln 2}{\mu} \tag{1}$$

$$HVL_2 = d_{1/4} - HVL_1 = \frac{\ln 4}{\mu} - HVL_1 \tag{2}$$

where μ is the linear attenuation coefficient of the absorber material, $d_{1/2}$ and $d_{1/4}$ are the absorber thicknesses which attenuate the primary beam intensity (i.e. air kerma rate) to half and to quarter of the initial value, respectively. By comparing the values of the first and second HVL the homogeneity coefficient h is defined [1].

Nikola Kržanović is with the Vinča Institute of Nuclear Sciences – National Institute of the Republic of Serbia, Department of Radiation and Environmental Protection, University of Belgrade, 12-14 Mike Petrovića Alasa, 11351 Vinča, Belgrade, Serbia (krzanovic@vin.bg.ac.rs)

Miloš Živanović is with the Vinča Institute of Nuclear Sciences – National Institute of the Republic of Serbia, Department of Radiation and Environmental Protection, University of Belgrade, 12-14 Mike Petrovića Alasa, 11351 Vinča, Belgrade, Serbia (milosz@vin.bg.ac.rs)

Olivera Ciraj-Bjelac is with the School of Electrical Engineering, University of Belgrade, 73 Bulevar Kralja Aleksandra, 11020 Belgrade, Serbia; Vinča Institute of Nuclear Sciences – National Institute of the Republic of Serbia, Department of Radiation and Environmental Protection, University of Belgrade, 12-14 Mike Petrovića Alasa, 11351 Vinča, Belgrade, Serbia (ociraj@vin.bg.ac.rs)

Predrag Božović is with the School of Electrical Engineering, University of Belgrade, 73 Bulevar Kralja Aleksandra, 11020 Belgrade, Serbia; Vinča Institute of Nuclear Sciences – National Institute of the Republic of Serbia, Department of Radiation and Environmental Protection, University of Belgrade, 12-14 Mike Petrovića Alasa, 11351 Vinča, Belgrade, Serbia (bozovic@vin.bg.ac.rs)

Andrea Kojić is with the Faculty of Physics, University of Belgrade, 12 Studentski Trg, 11001 Belgrade, Serbia; Vinča Institute of Nuclear Sciences – National Institute of the Republic of Serbia, Department of Radiation and Environmental Protection, University of Belgrade, 12-14 Mike Petrovića Alasa, 11351 Vinča, Belgrade, Serbia (andrea.kojic@vin.bg.ac.rs)

$$h = \frac{HVL_1}{HVL_2} \quad (3)$$

In the previous research regarding characterization of the diagnostic radiology X-ray fields, the first and second HVL and the homogeneity coefficient were determined only for a part of the RQR series, due to the available radiation qualities at the SSDL at the time [4]. Following the previous characterization procedure the old X-ray generator Phillips MG320 has been replaced by the current Hopewell Designs X80-225 kV-E generator, requiring new characterization procedure of the diagnostic radiology X-ray fields.

In this paper values of the first and second HVL are determined in order to establish the RQR series in the Vinca Institute of Nuclear Sciences Secondary Standard Dosimetry Laboratory (SSDL).

II. Materials and Methods

The RQR radiation quality series is used for the calibration of dosimetry equipment which would be used under clinical conditions that correspond to various radiography and fluoroscopy procedures. These radiation qualities are based on X-ray tube voltages in the range from 40 kV up to 150 kV. In Table 1, the properties of RQR radiation qualities in terms of X-ray tube voltage, first HVL and homogeneity coefficient are displayed [1].

TABLE I
Radiation beam emerging from X-ray assembly (RQR) radiation quality properties used for calibration of the QA dosimeters [1].

Radiation quality	*U* [kV]	1st HVL [mm Al]	*h*
RQR2	40	1.42	0.81
RQR3	50	1.78	0.76
RQR4	60	2.19	0.74
RQR5	70	2.58	0.71
RQR6	80	3.01	0.69
RQR7	90	3.48	0.68
RQR8	100	3.97	0.68
RQR9	120	5.00	0.68
RQR10	150	6.57	0.72

The diagnostic radiology beams were characterized for the Hopewell Designs X80-225 kV-E X-ray generator which operates in the continuous mode. The HVL measurements were performed by using the 3.6 cm^3 secondary standard spherical ionization chamber Exradin A3 (Standard Imaging) with the UNIDOS Webline (PTW) electrometer. The ionization chamber was calibrated together with the electrometer in the IAEA Dosimetry Laboratory, establishing traceability to the primary standard for all the RQR series radiation qualities. The reference radiation quality in the RQR series is the RQR5 radiation quality. The standard ionization chamber has negligible energy response dependence over a wide energy range, not requiring correction factors for this influence quantity.

The ionization chamber is positioned at the distance specific for the calibration of the dosimetry equipment, being 100 cm. Owing to the fact that the fluctuations in the output of the X-ray generator lead to variations in the measured air kerma rate values, a correction for these variations is needed. In order to correct the X-ray output variation, a plane-parallel transmission ionization chamber is positioned after the filtration of the primary radiation beam. The PTW 34014 ionization chamber with the PTW UNIDOS electrometer has been used for the charge measurements during the air kerma rate measurements with the reference standard.

The additional filtration absorbers are placed equidistantly from the ionization chamber and the monitor chamber in order to minimize the effects of scattered radiation during the HVL measurements. The aperture at the position of the aluminum absorbers has a diameter of 3.8 cm, leading to the field diameter at the point of test of 5.8 cm. The distances between the ionization chamber and the absorber and between the absorber and the monitor chamber were 34 cm, which is greater than five times the field diameter at the point of test. By ensuring that this condition is fulfilled, the production of scattered radiation from the aluminum absorber is negligible, and the contribution of this radiation to the measured signal of the ionization chamber and the monitor chamber is minimized.

The measurement set-up for the HVL measurements is displayed in Fig. 1, while the image in which the ionization chamber, aperture where additional filtration is placed and the X-ray generator are displayed in Fig. 2.

The first and second HVL were estimated by successively increasing the additional filtration aluminum absorber thickness, and measuring the air kerma rate. All of the air kerma values were compared to the initial air kerma rate value measured when no additional filtration has been added. In order to determine the attenuation curves for all of the radiation qualities, aluminum absorber thicknesses ranging from 0.7 mm to 20.0 mm were used. Since the air density represents an important influence quantity for the air kerma measurements, all of the standard and monitor ionization chamber measurements were corrected for the ambient conditions (the effects of ambient temperature and pressure).

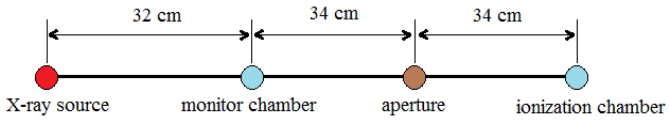

Fig. 1. Measurement set-up for the HVL measurements. The aperture where the additional aluminum filtration is added is positioned equidistantly between the ionization chamber and the monitor chamber, due to the minimization of the scattered radiation contribution. The ionization chamber is placed on the calibration distance of 100 cm from the X-ray source.

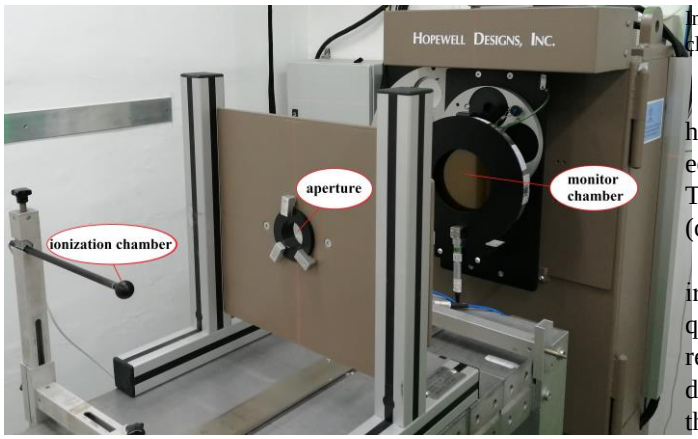

Fig. 2. HVL measurement set-up with indicated ionization chamber, monitor chamber and the aperture where the additional aluminum filtration of various thicknesses was positioned.

III. RESULTS AND DISCUSSION

For all the RQR radiation qualities the attenuation curve (according to the exponential attenuation law in the absorber material) has been recorded. The aluminum filter thicknesses were successively increased, where the filter thickness increase steps near the absorber thicknesses that correspond to the targeted HVL values given in the standard [1] [2] were smaller.

Due to the beam hardening the HVL cannot be estimated by performing the attenuation curve fitting over the whole dataset, therefore the first and second HVL were determined by performing interpolation of the data for the absorber thicknesses near the expected HVL values. In Figure 3 the recorded attenuation curve for the RQR5 radiation quality is displayed. All of the air kerma rate values were corrected for the influence of the X-ray generator output variations and normalized to the values measured when no additional filtration was added at the position of the aperture, for each radiation quality separately.

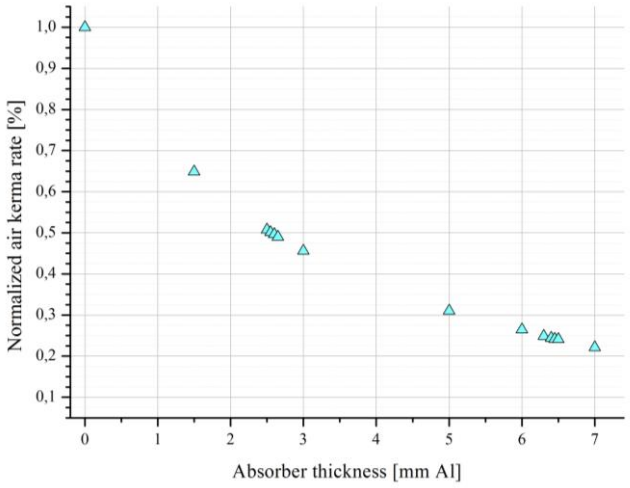

Fig. 3. Attenuation curve recorded for the RQR5 radiation quality. Air kerma rate was corrected for the output variation of the X-ray generator and normalized to the value with no added filtration at the aperture position. Increased number of data points was measured for the aluminum thicknesses close to the HVL standard values [1].

The first and second HVL values were estimated, and the homogeneity coefficient has been determined by using the equations 1-3. The obtained HVL values are displayed in Table 2, along with the deviations from the reference values (displayed in Table 1).

Deviation of the measured first HVL from the values given in IEC 61267 [2] is less than ±5% for all the radiation qualities in the RQR series. The lowest deviation from the reference HVL value was determined for the reference diagnostic radiology radiation quality RQR5 (-0.4%), while the largest deviation from the standard was recorded for the RQR9 and RQR10 radiation qualities. Regarding the second HVL and the homogeneity coefficient, the largest deviation from the standard [2] values is observed for the RQR4 radiation quality, while there was no deviation of the homogeneity coefficient determined for the RQR3 and RQR7 radiation qualities.

TABLE II
ESTIMATED FIRST AND SECOND HVL VALUES AND THE HOMOGENEITY COEFFICIENTS FOR THE RQR RADIATION QUALITIES, AND THE DEVIATIONS FROM THE REFERENCE VALUES.

Radiation quality	HVL_1	HVL_2	h	$\Delta(d_{1/2})$ [%]	$\Delta(h)$ [%]
RQR2	1.40	1.78	0.79	-1.4	-2.5
RQR3	1.77	2.34	0.76	-0.6	0.0
RQR4	2.17	3.04	0.71	-0.9	-4.1
RQR5	2.57	3.69	0.70	-0.4	-1.4
RQR6	3.06	4.33	0.71	1.7	2.9
RQR7	3.55	5.26	0.68	2.0	0.0
RQR8	4.01	6.08	0.66	1.0	-2.9
RQR9	5.13	7.70	0.67	2.6	-1.5
RQR10	6.85	9.43	0.73	4.3	1.4

Considering the criteria set by the standard [1] [2], the primary beam specifying quantities (X-ray tube voltage and the first HVL) should be adjusted as closely as possible to the values presented in Table 1, in such a way that the ratio of air kerma rate with and without additional filtration at the aperture position is in the range 0.485 - 0.515. If the estimated air kerma ratio for the given HVL lies slightly out of the given range, additional filtration thickness correction may be needed. The maximum deviation for the secondary beam specifying quantity (homogeneity coefficient) is ±0.03 from the values given in Table 1 for each of the radiation qualities.

The measured air kerma rate values for added filtration corresponding to the first HVL, as well as the estimated values of homogeneity coefficient, were in accordance with the standard.

IV. Conclusion

The Secondary Standard Dosimetry Laboratory represents an important element in enforcing the metrology traceability chain, improving the quality of dosimetry measurements in diagnostic radiology by performing adequate calibration procedures in the reference radiation fields established according to the IEC standard. The first and second HVL measurement results would contribute to the eventual corrections of the manufacturer preset X-ray beam filtrations in order to reduce the deviation from the standard HVL and homogeneity coefficient values, ensuring that the X-ray spectra are quantitatively well characterized. Employing characterized X-ray fields for diagnostic radiology improves the calibration and testing procedures of dosimetry equipment designated for the use under medical irradiation conditions. Furthermore, future introduction of new radiation qualities with X-ray tube voltages and filtrations in close correspondence with clinical conditions, and establishing these new radiation qualities in SSDLs would result in improvement of dosimetry equipment accuracy on-site.

Acknowledgment

This research was funded by the Ministry of Education, Science and Technological Development of the Republic of Serbia.

References

[1] *Dosimetry in Diagnostic Radiology: An International Code of Practice*, IAEA TRS 457, 2007.

[2] *Medical diagnostic X-ray equipment - Radiation conditions for use in the determination of characteristics*, IEC 61267, 2005.

[3] O. Ciraj-Bjelac, N. Kržanović, M. Živanović, V. Blideanu, F. De Monte, M. Deleu, A. Feghalli Joelle, A. Gallagher, Ž. Knežević, C. Maccia, F. Malchair, J. Plagnard, M. Sans Merce, G. Simantirakis, J. Dabin, „VERIDIC: Validation and estimation of radiation skin dose in interventional cardiology“, XXX Simpozijum DZZSCG, Divčibare, Srbija, pp. 386-392, 2nd-4th October, 2019.

[4] D. Čekerevac, O. Ciraj-Bjelac, M. Živanović, P. Božović, “Uspostavljanje standardnih kvaliteta snopa u SSDL za primenu u oblsati dijagnostičke radiologije”, XXVI Simpozijum DZZSCG, Tara, Srbija, pp. 229-233, 12th-14th October, 2011.

Uporedna analiza uticaja γ i X zračenja na karakteristike komercijalnih gasnih odvodnika prenapona u impulsnom režimu rada

Luka Rubinjoni, Srboljub Stanković, Tomislav Stojić, Boris Lončar

***Apstrakt*—Gasni odvodnici prenapona su izdržljive i pouzdane komponente za bezbedno odvođenje prenapona, koje rade na principu jonizacije izolacionog medijuma – gasa. Jonizujuće zračenje utiče na karakteristike odvodnika. U ovom radu prikazana je uporedna analiza uticaja uticaja γ i X zračenja na osobine komercijalnih gasnih odvodnika prenapona u impulsnom režimu rada, primenom poluempirijske metode merenja impulsnog probojnog napona i određivanja impulsne (volt-sekundne) karakteristike.**

***Ključne reči*— Gasni odvodnik prenapona; γ zračenje; X zračenje; radijaciona otpornost.**

I. UVOD

Prenapon nastaje kada potencijal jedne tačke nekog voda, uređaja ili komponente postane veći od dozvoljenog, u odnosu na drugu tačku u kolu ili tačku nultog potencijala. U zavisnosti od stepena prekoračenja, prenapon može dovesti do privremenog ili trajnog poremećaja u radu uređaja, oštećenja uređaja, čak i ugroziti bezbednost osobe koja rukuje uređajem u trenutku nastanka prenapona. Prenaponi mogu biti impulsni ili trajni. Nastaju direktno usled komutacijskih procesa (poput uključivanja ili isključivanja uređaja, promena režima rada elektromotora i slično), elektrostatičkog pražnjenja i atmosferskog pražnjenja unutar uređaja ili komponente, ili unutar mreže na koju su uređaji priključeni; ili indirektno, kao posledica interakcije provodnika (žičanih struktura komponente ili uređaja) sa elektromagnetnim impulsom. Atmosferska pražnjenja (munje i gromovi) su najopasniji izvor prenapona, jer se ne može uticati na uzrok njegovog nastanka[1].

Gasni odvodnici prenapona (eng. *Gas Filled Surge Arresters* – GFSA) su komponente za prenaponsku zaštitu koje se sastoje od dve ili tri elektrode u simetričnoj konfiguraciji, zatopljene u keramičko ili stakleno kućište ispunjeno izolacionim medijumom – plemenitim gasom (najčešće argon) sa određenim primesama. Pri nastanku prenapona dolazi do jonizacije gasa i posledičnog naglog pada električnog otpora komponente, koji omogućava bezbedno odvođenje prenapona mimo osetljivih delova mreže ili uređaja. Gasne odvodnike prenapona odlikuje velika izdržljivost i sposobnost odvođenja vrlo velikih struja (do 60 kA, za pojedine komponente), ali se suočavaju sa malom brzinom reagovanja u odnosu na druge tipove odvodnika prenapona, i problemom gašenja odvodnika u impulsnom režimu.

U ovom radu predstavljeni su rezultati ispitivanja karakteristika komercijalnih gasnih odvodnika prenapona, proizvođača Simens i Citel, u impulsnom režimu rada, u polju γ i X zračenja.

Luka Rubinjoni – Inovacioni centar Tehnološko-metalurškog fakulteta, Karnegijeva 4, 11120 Beograd, Srbija (e-mail: rubinjoni@tmf.bg.ac.rs).

Srboljub Stanković – Institut za nuklearne nauke "Vinča", Univerzitet u Beogradu, Mike Petrovića Alasa 12-14, 11351 Vinča, Beograd, Srbija (e-mail: srbas@vin.bg.ac.rs).

Tomislav Stojić – Mašinski fakultet, Univerzitet u Beogradu, Kraljice Marije 16, 11120 Beograd, Srbija (e-mail: tstojic@mas.bg.ac.rs).

Boris Lončar – Tehnološko-metalurški fakultet, Univerzitet u Beogradu, Karnegijeva 4, Beograd, Srbija (e-mail: bloncar@tmf.bg.ac.rs).

II. IMPULSNA KARAKTERISTIKA ODVODNIKA PRENAPONA

Impulsna (volt-sekundna) karakteristika prikazuje probojni napon gasne elektrodne konfiguracije u funkciji vremena trajanja primenjenih naponskih impulsa. Egzaktno eksperimentalno određivanje impulsne karakteristike zahteva veliki broj aktivacija korišćenjem naponskih impulsa različitih oblika. S druge strane, primenom zakona površina moguće je odrediti impulsnu karakteristiku samo na bazi jedne serije merenja (korišćenjem jednog oblika naponskog impulsa). Polazna tačka za izvođenje zakona površina je pretpostavka da se brzina kojom se širi plazma u međuelektrodnom prostoru linearno povećava sa jačinom električnog polja [2]:

$$v(x,t) = k\left[E(x,t) - E_s(x)\right] \tag{1}$$

gde je k – konstanta koja zavisi od mehanizma električnog pražnjenja i polariteta elektroda. Es je nazivna jačina polja, koja odgovara nazivnoj vrednosti probojnog napona Us.

Pošto jednosmerni probojni napon u(t) predstavlja najmanju moguću vrednost probojnog napona za specifičnu elektrodnu konfiguraciju, uslov da dođe do impulsnog proboja je da napon bude veći od nazivnog napona Us.

Pod pretpostavkom zanemarivanja prostornog opterećenja u međuelektrodnom prostoru jačina električnog polja se može napisati kao:

$$E(x,t) = u(t)\cdot g(x) \tag{2}$$

gde je g(x) funkcija koja zavisi od geometrijskih uslova i određena je geometrijom elektrodne konfiguracije.

Odavde je zamenom (2) u (1):

$$v(x,t) = \frac{\mathrm{d}x}{\mathrm{d}t} = K\cdot g(x)\cdot\left[u(t) - U_s\right] \tag{3}$$

Korišćenjem izraza za srednju vrednost električnog polja:

$$\overline{E} = \frac{1}{d}\int_0^d E_s(x)\,dx = \frac{U_s}{d} \tag{4}$$

i jednačina:

$$\frac{1}{d}\int_0^d g(x)\mathrm{d}x = \frac{1}{d} \tag{5}$$

$$\frac{E_s(x)}{g(x)} = U_s \tag{6}$$

dobijamo:

$$v(x,t) = K \cdot g(x) \cdot \left[u(t) - \frac{E_s(x)}{g(x)} \right] \tag{7}$$

Razdvajanjem promenljivih i integracijom konačno dobijamo [51]:

$$\frac{1}{k}\int_{x=0}^{x=x_k} \frac{\mathrm{d}x}{g(x)} = \int_{t_1}^{t_1+t_a} [u(t) - U_s]\mathrm{d}t = P = \text{const} \tag{8}$$

gde x=xk predstavlja tačku u kojoj *Townsend*–ov mehanizam pražnjenja prelazi u strimerski, a $t = t_1 + t_a$ je odgovarajući vremenski trenutak. U skladu sa izrazom (8) u kome je prvi integral – integral rastojanja, a drugi integral po vremenu, sledi da se konstantna geometrijska površina mora formirati u naponsko – vremenskoj ravni između u(t) i U_s, kako bi moglo da dođe do proboja. Pošto površina P i vrednost statičkog probojnog napona, kao karakteristike izolacije ne zavise od primenjenog napona, sledi da je poznavanje ove dve veličine dovoljno za izračunavanje impulsne karakteristike i impulsnog probojnog napona[3].

Nakon dovoljnog broja merenja statičkog probojnog napona (najmanje 20) i impulsnog probojnog napona (najmanje 50), na osnovu funkcije raspodele verovatnoće mogu se odrediti granice oblasti impulsne karakteristike U_x i U_y u procentima (najčešće se uzima x = 0,1%, y = 99,9%)[4]. Sa granicama određenim na ovaj način i uz poznavanje vrednosti statičkog probojnog napona može se rešiti sledeći sistem jednačina:

$$\begin{aligned} u(t) &= U_s, \quad t = t_1 \\ u(t) &= U_x, \quad t = t_{ax} \\ u(t) &= U_y, \quad t = t_{ay} \end{aligned} \tag{9}$$

Vrednosti t_1, t_{ax}, t_{ay} omogućavaju da se primenom zakona površina odrede odgovarajuće površine P_x i P_y:

$$\begin{aligned} P_x &= \int_{t_1}^{t_1+t_{ax}} [u(t) - U_s]\mathrm{d}t = \text{const} \\ P_y &= \int_{t_1}^{t_1+t_{ay}} [u(t) - U_s]\mathrm{d}t = \text{const} \end{aligned} \tag{10}$$

Kada su određene površine P_x i P_y moguće je korišćenjem zakona površina odrediti x-ta i y-ta granica opsega slučajne promenljive "impulsni probojni napon" za ma koji oblik napona u(t). Ako se oblik tog napona uzme kao parameter u određenom vremenskom intervalu moguće je odrediti impulsne karakteristike.

III. MATERIJAL I EKSPERIMENT

Merenja su vršena na sledećim komercijalnim komponentama: 1) SIEMENS gasni odvodnici nominalnog napona 230 V, 2) CITEL BB bipolarni keramički gasni odvodnici jednosmernog prenapona 230 V. Spoljašnje dimenzije i oblik svih SIEMENS, odnosno CITEL komponenti su bili isti. Sva merenja su vršena na temperaturi od 20 °C u Metrološko – dozimetrijskoj laboratoriji Laboratorije za zaštitu od zračenja i zaštitu životne sredine Instituta za nuklearne nauke Vinča.

Instrumentacija korišćena u eksperimentalnim ispitivanjima u impulsnom režimu sastojala se od sledećih osnovnih delova:

1) komercijalni odvodnici SIEMENS i CITEL;
2) gasno – vakuumska komora;
3) impulsni test generator Haefely tip P6T VF-tel 202671 sa priborom;
4) osciloskop Tektronix TDS 220 SNB036675;
5) izolacioni transformator Elektron Zagreb;
6) koaksijalni kablovi i priključci.

Blok šema eksperimentalne postavke prikazana je na Sl. 1.

Uticaj γ zračenja na komercijalne GFSA komponente određivan je u polju ^{60}Co, primenom izvora uređaja IRPIK-B. Jačina apsorbovane doze iznosila je 96 cGy/h, 960 cGy/h i 1920 cGy/h, sa jačinom ekspozicione doze od $7{,}17*10^{-6}$ C/kgs, $7{,}17*10^{-5}$ C/kgs i $1{,}43*10^{-4}$ C/kgs.

Uticaj X zračenja na komercijalne GFSA komponente određivan je u poljima generisanim uređajem Philips MG-320, sa sledećim parametrima: napon X cevi 60 kV, 150 kV i 300 kV; struja cevi 15 mA, 10 mA i 10 mA (respektivno); energija X zraka 45 kEv, 115 kEv i 250 kEv, uz primenu filtracije prema ISO standardima. Jačina ekspozicione doze iznosila je $2{,}83*10^{-6}$ C/kgs, $5{,}89*10^{-6}$ C/kgs i $3{,}45*10^{-6}$ C/kgs.

Nakon kondicioniranja elektrodnog sistema (10-15 proboja sa pauzom od 30 sekundi između proboja), izvršeno je po 50 merenja probojnog napona u impulsnom režimu rada, za tri brzine impulsa, i to: 1,2/50 μs, 10/700 μs i 100/700 μs.

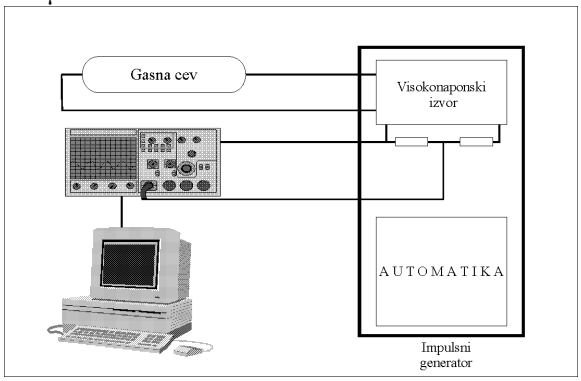

Sl. 1. Blok šema opreme za eksperimentalna ispitivanja

IV. REZULTATI I DISKUSIJA

Statističkom obradom utvrđenih vrednosti probojnog napona konstruisana je impulsna (volt-sekundna) karakteristika gasnih odvodnika prenapona, primenom algoritma za poluempirijsko određivanje impulsne karakteristike[3]. Impulsna karakteristika za Citel odvodnike prikazana je na Sl. 2 i 3, a za Siemens odvodnike na Sl. 4 i 5.

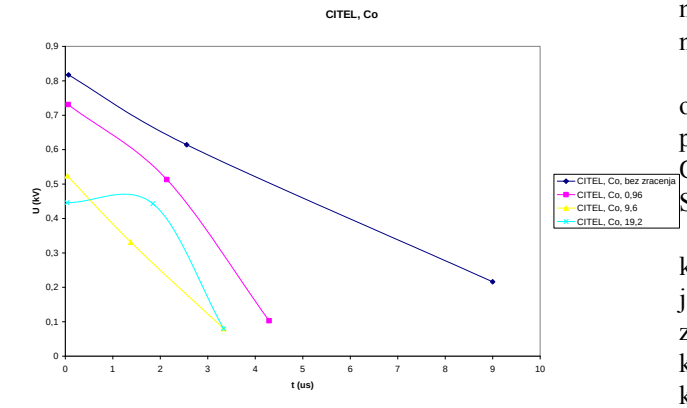

Sl. 1. Volt – sekundne karakteristike za CITEL komponente u polju γ zračenja.

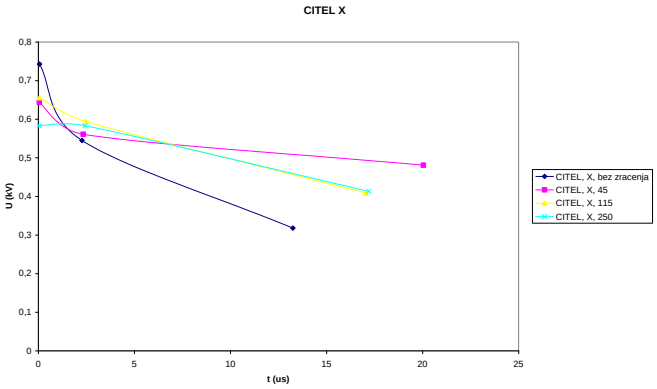

Sl. 2. Volt – sekundne karakteristike za CITEL komponente u polju X zračenja.

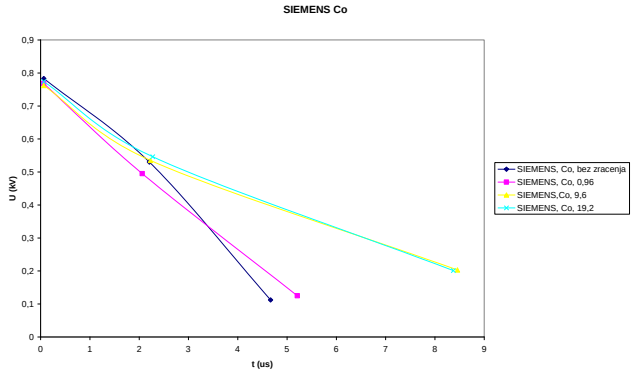

Sl. 3. Volt – sekundne karakteristike za SIEMENS komponente u polju γ zračenja.

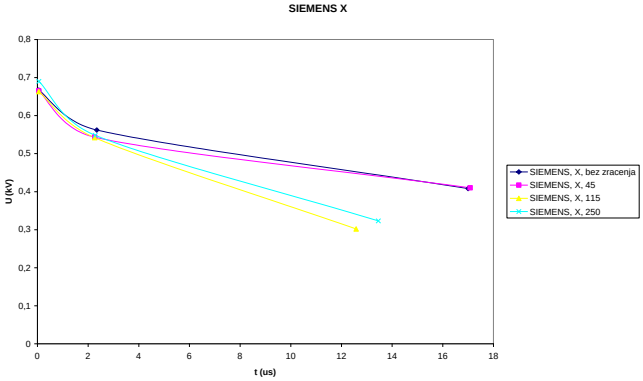

Sl. 4. Volt – sekundne karakteristike za SIEMENS komponente u polju X zračenja.

Sa prikazanih grafika možemo zaključiti sledeće:

1) Najmanje rasipanje vrednosti probojnog napona je pri najbržim korišćenim impulsima 1,2/50 μs, a najveće pri najsporijim impulsima 100/700 μs.

2) Gama zračenje utiče na karakteristike odvodnika, ali se one ne menjaju po nekoj utvrđenoj zakonitosti sa povećanjem jačine doze. Jedino možemo zaključiti da kod CITEL komponenti dolazi do neznatnog poboljšanja, a kod SIEMENS komponenti do pogoršanja karakteristika.

3) X zračenje mnogo manje od gama zračenja utiče na karakteristike pomenutih komercijalnih odvodnika. Pri tom je očigledno da kod CITEL komponenti u polju gama zračenja dolazi do degradacije njihovih performansi, dok kod SIEMENS komponenti dolazi do poboljšanja karakteristika (to jedino ne važi pri najsporijim impulsima). Možemo reći da je uticaj X zračenja na odvodnike neznatan.

Zaključak

V. ZAKLJUČAK

Dobijeni rezultati ukazuju na to da su u polju gama zračenja otporniji Citel, a u polju X zračenja Siemens komercijalni odvodnici. Sve uočene promene su reverzibilnog karaktera, i nakon određenog perioda vremena i Citel i Siemens komponente ponovo imaju iste performanse, kao pre dejstva zračenja, to jest, karakteriše ih dinamička radijaciona otpornost.

ZAHVALNICA

Ovaj rad napisan je u okviru projekata Ministarstva prosvete, nauke i tehnološkog razvoja ON171007 i III 43009.

LITERATURA

[1] B. Lončar, „Radijaciona otpornost memorijskih i prenaponskih zaštitnih komponenata“, doktorska disertacija, ETF, BU, Beograd, Srb. 2003.

[2] P. Osmokrović, G. Đogo, "Applicability of simple expressions for electrical breakdown probability in vacuum," *IEEE Trans Electr Insul*, vol. 24, no. 6, pp. 943-948, 1989.

[3] P. Osmokrović, B. Lončar, S. Stanković, "The new method of determining characteristics of elements for over-voltage protection of low-voltage system," *IEEE Trans on Instrum Meas*, vol. 55, no. 1, pp. 257-265, 2006.

[4] W. Hauschild and W. Mosch, *Statistik für Elektrotechniker*, Berlin: VEB Verlag Technik, 1984.

ABSTRACT

Gas filled surge arresters are durable and reliable components for safe overvoltage conduction, that operate on the principle of ionization of the isolation medium – gas. Ionizing radiation impacts the properties of the arrester. This paper reports a comparative analysis of the effect of γ and X irradiation on the properties of commercial gas filled surge arresters in impulse operation mode, by application of a semiempiric method of measurement of impulse breach voltage and determination of the impulse (volt-second) characteristic.

Comparative analysis of the effect of γ and X radiation to properties of commercial gas filled surge arresters in impulse mode

Luka Rubinjoni, Srboljub Stanković, Tomislav Stojić, Boris Lončar

Uncertainty budget for Ambient Dose Equivalent Rate Measurements with Energy – compensated GM Counters

Jelena Krneta Nikolić*, Ivana Vukanac, Miloš Živanović, Milica Rajačić, Dragana Todorović, Gordana Pantelić and Marija Janković

***Abstract*— Dosimetric measurements are readily used to assess the exposure of public and working force to ionizing radiation via monitoring various spaces and goods that are imported or in transit through the country. This is done by measuring the ambient dose equivalent rate on the surface of the goods, in the transportation vehicle, or inside of the object of interest. The instruments that are often used in this monitoring type of measurement are compensated Geiger-Muller tube counters. The indication of these instruments is often count per second (cps) and therefore it has to be multiplied by calibration coefficient to obtain result in Sv/h. Due to this and due to the nature of the measurement itself, the greatest challenge is to define the uncertainty budget and calculate the measurement uncertainty accordingly. In this paper we will present the analysis of the uncertainty budget for 4 types of dosimeters used in Radiation and Environmental Protection Department, their calculated measurement uncertainty and the comparison conducted between our instruments and other calibrated instruments that are in the quality management system.**

***Index Terms*— dosimetry; uncertainty budget; measurement uncertainty**

I. Introduction

Dosimetric measurements are in wide use in radiation protection, aimed both at continuous control of medical instruments that are using the ionizing radiation sources and exposure of patients and staff operating those instruments [1]. Also, dosimetric measurements are readily used to assess the exposure of public and working force to ionizing radiation via screening of various spaces and goods that are imported or in transit through the country [2, 3]. This is done by measuring the ambient dose rate equivalent, $H^*(10)$, on the surface of the goods, in the transportation vehicle, or inside of the object of interest – ambient monitoring.

Dosimeters used for ambient monitoring are often based on compensated Geiger-Muller tubes, and most of these instruments used in Radiation and Environmental Protection Department in the Institute for Nuclear Sciences Vinča, are made inhouse. Ambient dose equivalent rate is the quantity that is used for ambient monitoring and it is expressed in unit sievert per hour (Sv/h). Many ambient monitors have indication directly in Sv/h, but other instruments have indication in counts per second (cps) and the values in terms of ambient dose equivalent need to be calculated based on the calibration coefficient [4]. Due to this and due to the nature of the measurement itself, the greatest challenge is to define the uncertainty budget and calculate the measurement uncertainty accordingly.

The uncertainty budget has to include all the contributions to the uncertainty that may arise from the fact that, unlike during the calibration in reference fields, radiation energy, angle of incidence and dose rate are unknown. Therefore, the position of the instrument with respect to the source, the distance from the source and the discrepancy of measured radiation fields in comparison to those used for calibration of the instrument, can greatly influence the result.

In this paper we will present the analysis of the uncertainty budget for 4 types of dosimeters used in Radiation and Environmental Protection Department, their calculated measurement uncertainty and the comparison conducted between our instruments and other calibrated instruments that are in the quality management system.

II. Main Results and Discussion

In the Radiation and Environmental Protection Department of the Institute for Nuclear Sciences Vinča, the instruments used for dosimetry are produced inhouse. The following types of instruments will be analyzed: MOKO-100, KOMO-100 RMK 10 and RMK-10P (total of 10 instruments). These instruments have an indication in cps and therefore the indication has to be multiplied by a calibration coefficient to produce results in Sv/h. However, the position of the instrument in relation to the examined

Jelena Krneta Nikolić is with the University of Belgrade, Institute for Nuclear Sciences Vinča, National Institute of Republic of Serbia, Radiation and Environmental Protection Department Mike Petrovića Alasa 12-14, Vinča 11000 Belgrade, Serbia (e-mail: jnikolic@ vin.bg.ac.rs).

Ivana Vukanac is with the University of Belgrade, Institute for Nuclear Sciences Vinča, National Institute of Republic of Serbia, Radiation and Environmental Protection Department Mike Petrovića Alasa 12-14, Vinča 11000 Belgrade, Serbia (e-mail: vukanac@ vin.bg.ac.rs)

Miloš Živanovic is with the University of Belgrade, Institute for Nuclear Sciences Vinča, National Institute of Republic of Serbia, Radiation and Environmental Protection Department Mike Petrovića Alasa 12-14, Vinča 11000 Belgrade, Serbia (e-mail: milosz@ vin.bg.ac.rs)

Milica Rajačić is with the University of Belgrade, Institute for Nuclear Sciences Vinča, National Institute of Republic of Serbia, Radiation and Environmental Protection Department Mike Petrovića Alasa 12-14, Vinča 11000 Belgrade, Serbia (e-mail: milica100@ vin.bg.ac.rs)

Dragana Todorović is with the University of Belgrade, Institute for Nuclear Sciences Vinča, National Institute of Republic of Serbia, Radiation and Environmental Protection Department Mike Petrovića Alasa 12-14, Vinča 11000 Belgrade, Serbia (e-mail: beba@ vinca.bg.ac.rs)

Gordana Pantelić is with the University of Belgrade, Institute for Nuclear Sciences Vinča, National Institute of Republic of Serbia, Radiation and Environmental Protection Department Mike Petrovića Alasa 12-14, Vinča 11000 Belgrade, Serbia (e-mail: pantelic@ vin.bg.ac.rs)

Marija Janković is with the University of Belgrade, Institute for Nuclear Sciences Vinča, National Institute of Republic of Serbia, Radiation and Environmental Protection Department Mike Petrovića Alasa 12-14, Vinča 11000 Belgrade, Serbia (e-mail: marijam@ vin.bg.ac.rs)

objects, the energy emitted from the present radionuclides, as well as overall conditions of the measurement can widely differ from the conditions in which the calibration was performed. That is why the uncertainty budget has to contain not only the contribution from the calibration factor itself, but contributions from other parameters that are influencing the measurement result. The task of defining the contributions and measuring the value of each contribution to the measurement uncertainty is by definition an uncertainty budget.

A. Uncertainty budget

The first contribution to the uncertainty budget is the calibration factor. The calibration is performed in the Secondary Standards Calibration Laboratory in the Radiation and Environmental Protection Department by using the sources with the defined radiation quality, angle of incidence and dose rate. Calibration coefficient is then defined as the ratio of the refrence value and the indication of the instrument. The calibration coefficient with the appropriate measurement uncertainty is stated in a Calibration certificate. Exact functional dependence of calibration factor on radiation energy, dose rate and angle is not known and is different for each type of the dosimeter (depending on the tube, casing, additional energy compensation filters, software corrections, e.g. for dead time, etc). Furthermore, even if this was known, analytical treatment of uncertainty would be hard or impossible, especially in case of energy dependence, because the radiation is not monoenergetic, but is instead covering a wide spectrum, with unknown distribution. Because of this, it is assumed that energy, dose rate and angle can be anywhere in the defined ranges (ranges are appropriate for the planned use of the dosimeters). In this case, worst case scenario is used – maximum variation of calibration factor with energy, angle and dose rate and rectangular distribution, which is wider than normal or triangular.

After the calibration coefficient is determined, the linearity of the instrument response has to be evaluated. It is done by exposing the instrument to the different dose equivalent rates produced by the same or different reference source. The range of instrument calibration coefficients for different dose rates represents the range of linearity. Since it is assumed that the distribution of the results follows rectangular distribution, the range should be divided by 2 (to obtain the half range needed for the usual way of setting the uncertainty i.e. result ± half of the range) and then by 1.73 in order to obtain the standard measurement uncertainty with coverage factor 1.

Also, the repeatability of the measurement should be checked. For this purpose, we measured an enclosed point source containing ^{60}Co, product number 9031-OL-591/09 with activity of 732.9 kBq on 01.08.2011, produced by Czech Metrology Institute. Measurement was repeated 20 times and the standard deviation of the obtained values was calculated. This source and setup were chosen because the dose rate corresponds to the conditions occurring in routine dosimetry measurements.

Finally, the dependence of instrument response to different energies (qualities of the beam) and angles of incidence was estimated. Special attention was given to the range of energies. This should be as close as possible to the range of energies that are expected to be encountered in the real measurement situation. For this purpose, the sources containing ^{60}Co and ^{137}Cs were used, as well as radiation qualities from narrow series produced by an X-ray unit according to ISO 4037-1 [1]. Angular dependence was evaluated together with energy dependence, as is recommended by relevant IEC standards [5]. The range of responses for both different angles and different energies was recorded. Since the rectangular distribution was assumed, the range was divided by 2 and then by 1.73 for the rectangular distribution, in order to obtain the standard measurement uncertainty with coverage factor 1 [6].

Exact functional dependence of calibration factor on radiation energy, dose rate and angle is not known and is different for each type of the dosimeter (depending on the tube, casing, additional energy compensation filters, software corrections, e.g. for dead time, etc). Furthermore, even if this was known, analytical treatment of uncertainty would be hard or impossible, especially in case of energy dependence, because the radiation is not monoenergetic, but is instead covering a wide spectrum, with unknown distribution. Because of this, it is assumed that energy, dose rate and angle can be anywhere in the defined ranges (ranges are appropriate for the planned use of the dosimeters). In this case, worst case scenario is used – maximum variation of calibration factor with energy, angle and dose rate and rectangular distribution, which is wider than normal or triangular.

After all the contributions to the measurement uncertainty were identified and assessed, the expanded combined measurement uncertainty can be calculated using the following Equation [6]:

$$U = 2 \cdot \sqrt{\sum_i u_i^2} \cdot \qquad (1)$$

where U represents the expanded combined measurement uncertainty with coverage factor k=2 and u_i are individual contributions, as described in this section. It is assumed that all the contributions to the uncertainty have the same influence on the result, and that they are mutualy independent, all weighing factors are set to 1. Coverage factor 2 means that that the true value lies with approximately 95% confidence level within the range of the measured value ± given uncertainty (normal distribution is assumed for the combined uncertainty) .

B. Results and Discussion

The uncertainty budget contributions with the range of values obtained for each contribution is presented in Table I.

The values of the contributions to the uncertainty were obtained for each of 10 investigated instruments, using procedures described in previous section of the manuscript.

TABLE I
CONTRIBUTIONS TO THE MEASUREMENT UNCERTAINTY

Contribution	**Standard uncertainty range [%]**
Calibration factor	4.1 – 13.6
Linearity	1.0 – 5.8
Energy and angle	18.3 – 22.3
Repeatability	1.7-3.2
Expanded combined measurement uncertainty, coverage factor 2	40-51%

As it can be seen from the Table I, the range of different contributions is wide, but it is noticeable that the energy and angular dependence carries the largest part. It is to be expected, due to the construction of the counting tube itself. The repeatability test showed satisfying results, since the indication of the instruments did not vary significantly. Therefore, the contribution of the repeatability to the measurement uncertainty is only 2-3%.

Linearity proved to be quite stable for all instruments, contributing with 1.0-5.8% to the overall measurement uncertainty. This contribution is of the order of magnitude of the repeatability of measurements at a single dose rate, and as such, can be attributed to the stochastic nature of the interaction between the instrument and the radiation from the source.

The measurement uncertainty of the calibration factor is dependent on the process of the calibration and therefore can not be influenced directly. It contains within itself, all the contributions to the uncertainty that arises from the procedure of calibration.

When all the contributions are combined according to the Equation (1), the expanded combined measurement uncertainty ranges from 39.8% to 51.2%, for coverage factor 2. This quite large uncertainty is not unexpected in this kind of measurement as it can be seen from [5]. It is important to note that all the investigated properties of the 4 dosimeter types are within the limits defined by relevant international standard [1].

Additional check-up of the performance of some of the investigated instruments was conducted by comparison with other calibrated instruments that are in the quality management system (i.e. commercially available instruments used in other accredited laboratory, in this case Ionization chamber Cardinal, AD6 probe and Scintilation dosimeter ADb). The reported results, in form of mean value of 10 measurements with appropriate measurement uncertainty and also standard deviation of 10 measurements, are presented in Table II. The results of the comparison showed satisfactory agreement between the instruments, since all the reported results did not differ within the limits of the measurement uncertainty. Furthermore, the limits of acceptability of the results were set on 2 standard deviations of all reported results, calculated to be 0.27 μSvh-1 and all instruments produced acceptable results. This proved the accuracy of the measurements conducted using instruments for ambient monitoring.

TABLE II
CONTRIBUTIONS TO THE MEASUREMENT UNCERTAINTY

Instrument	**Measured dose [μSvh-1] 10 measurements per instrument**	
	Reported result	**Measurement uncertainty**
KOMO TL s/No. 001	2.23	1.07
Ionization chamber Cardinal 451P, s/No. 635	1.36	0.33
AD6 s/No. 109737	2.12	1.22
Scintilation dosimeter ADb, 109281	2.06	0.95
ATOMTEX AT6130	2.13	0.58
MOKO 100 s/No. 1802	2.14	0.92
RMK 10P s/No. 0412	2.12	1.10

III. CONCLUSION

In this paper we presented the analysis of the uncertainty budget for 4 types of dosimeters used in Radiation and Environmental Protection Department and their calculated measurement uncertainty. The scenario for which the uncertainty was estimated is measurement of dose rate in the field of unknown radiation source from unknown direction. The combined expanded uncertainty is between 40 and 51 percent, depending on the dosimeter type. The dosimeter properties giving rise to the measurement uncertainty are within the limits of tolerance given in IEC 60846-1 [5]. Although there are some contributions to the uncertainty that can not be influenced (such as the calibration factor and repeatability), there are some improvements that can be defined in the measurement in order to diminish, to a degree, some other contributions.

ACKNOWLEDGMENT

The research was funded by the Ministry of Education, Science and Technological Development of the Republic of Serbia.

REFERENCES

[1] *Radiological protection — X and gamma reference radiation for calibrating dosemeters and doserate meters and for determining their response as a function of photon energy — Part 1: Radiation characteristics and production methods*, ISO 4037-1:2019, 2019.

[2] Serbian radiation and nuclear safety and security Directirate "The law on radiation and nuclear safety and security" (Official gazette RS no. 95/18 i 10/19)

[3] Rulebook on Radioactivity Control of Goods During the Import, Export and Transit (Official Gazetteik RS 86/19)

[4] IAEA Safety Report Series No 16, *Calibration of radiation*

protection monitoring instruments, Vienna , Austria, IAEA, 2000
[5] International Electrotechnical Commission, *Radiation Protection Instrumentation - Ambient And/or Directional Dose Equivalent (Rate) Meters And/or Monitors for Beta, X and Gamma radiation - Part 1: Portable Workplace and Environmental Meters and Monitors*, IEC 60846-1, 2009
[6] *IAEA-TECDOC-1401, Quantifying uncertainty in nuclear analytical measurements*, Vienna, Austria, IAEA, 2004